

國立臺灣大學電機資訊學院電信工程學研究所

博士論文

Graduate Institute of Communication Engineering  
College of Electrical Engineering & Computer Science

National Taiwan University

Doctoral Dissertation

使用單埠量測結果重建多埠電路之散射矩陣

Multiport S-matrix Reconstruction Using One-Port  
Measurements

林沿鍾

Lin Yen-Chung

指導教授：瞿大雄 博士

Advisor: Chu Tah-Hsiung, Ph.D.

中華民國 104 年 6 月

June, 2015



國立臺灣大學博士學位論文  
口試委員會審定書

使用單埠量測結果重建多埠電路之散射矩陣  
Multiport S-matrix reconstruction using one-port  
measurements

本論文係林沿鍾君 (D97942009) 在國立臺灣大學電信工程學研究所完成之博士學位論文，於民國 104 年 6 月 26 日承下列考試委員審查通過及口試及格，特此證明

口試委員：

瞿大雄

(簽名)

(指導教授)

陳志榮

黃秉新

曾昭雄

蔡智明

陳志榮

吳宗霖

所長

(簽名)


## 誌謝



從碩士誌謝到博士誌謝，要感謝的人和事多了好多。寫論文的時候，總覺得一頁的空間好長，而寫誌謝時卻又突然變得好短。但願有緣讀到這篇誌謝的大家，能稍微感受到在這受限的文字背後，滿滿的感懷之意。

首先感謝最大力付出的瞿大雄教授，無論是實驗發想、技術乃至於文案，皆得力於老師的扶持才有今天的成果。而在學術之外，當我在生活上遇到難題時，瞿教授也盡力地協助，讓我更能穩定腳步。感謝季先生長年細心維持實驗室的正常運作，把精良的設備隨時保持在最佳狀態，讓我在截稿的關鍵時刻能專注於實驗內容，完全不用擔心儀器出狀況。感謝李偉強學長，雖然你不在實驗室已許久，但在理論發想初期及初次投稿論文時，你的鼓勵跟建議讓我安心不少。感謝張祐宸同學在重要時刻提供的實務技術指導。另外特別感謝我的電磁學啟蒙老師蔡智明教授，在虛度了廿年之後，我才終於在您的課堂上首次從『學』窺見了『思』的輪廓。得知您即將出任口試委員，也在我們這群大學同儕間引起一陣小騷動。而能在您的認可之下取得學位對我更是意義非凡。

感謝家鄉父親的資助，母親的支持。隨著接觸的事物越來越多，才能體會過去你們所維繫的穩定環境，對於一個人的影響有多麼巨大。感謝你們給過的那些日子，遠超過任何物質所能代表。並期許我們都能有足夠的智慧與勇氣，面對未來的任何挑戰。感謝大姊一家包括小愷替我分擔的憂慮。當我正在與論文水深火熱又面臨研發替代役的抉擇時，謝謝你們耐心地替我緩解心裡的不安。當然我也



不會忘記耘樂跟牧澄這兩顆小蘿蔔帶給大家的歡樂（！？），未來還請不要吝嗇地放下身段，無下限地賣萌吧！感謝林士恆在我最支不開身的時候，一肩負起照顧爸爸的责任。我一定要告訴你當我知道你要返回嘉義時，焦頭爛額的我是鬆了多麼大的一口氣。感謝堅不可摧 364 聯盟的蘇聖琪，林昱廷以及最接近第一線看我火燒屁股並且提供關鍵技術支援的黃品澄。感謝我的蘇曉芸，妳的一切決定都為了成就我的里程碑。只要是為了學業，對於我的任何提議一定是說不二全力配合，到了研究後期更是大量仰賴妳的資助。而當我的研究有了新的進展，妳就靜靜地聽我興奮的轉述。除了老師之外，就只有妳看著我把理論一層層建築起來，妳就是那位跟我并肩衝鋒的人。感謝蘇曉洳和蘇聖凱，謝謝你們過去十年來給了我這麼特别的回憶，從五月天、皮克斯、新台灣原味、555、廈門、上海到龜山島，無論到哪裡都留下了我們的足跡，大家合作把媽媽嚇到眼鏡噴發的那一天更是我們慶生成就的顛峰！是你們三姊弟一起把笑聲倒進我的生活裡。最後，謹以無限追思緬懷無緣見到此刻的長輩。我想我是少數能吃著岳母準備的便當做著研究的幸運兒，雖然只差一點，妳就能看到這一切，但我相信妳一定很驕傲妳的女婿終於順利完成了這個階段。願您在坎坷的一生之後能安息。謹將此微薄榮耀獻予您，以及所有我深切在乎的大家。

## 摘要



本論文提出以多個單埠之散射參數量測，據以重建多埠被動及主動電路之散射矩陣。降埠法係使用埠數少於  $n$  埠之網路分析儀，以獲得一  $n$  埠電路之散射矩陣，已知適用降埠法之網路分析儀埠數，最少為雙埠或三埠，本論文則將埠數進一步降至單埠，即最低埠數。

第二章闡述對一雙埠電路，如何使用輔助電路及單埠終端器，由多個單埠散射參數，重建該雙埠電路之散射矩陣。其重建結果進一步應用於降埠法，由多個單埠散射參數量測值，重建  $n$  埠電路之散射矩陣。由於使用單埠終端器，對於主動電路可能造成振盪，因此本章亦敘述雙埠主動電路之散射矩陣重建方法。最後，對於多埠互易電路，則提出可不使用降埠法，重建其  $n$  埠散射矩陣。

由於輔助電路在降低量測埠數至單埠極為重要，第三章則討論輔助電路之影響，藉由適當選擇輔助電路，可降低單埠量測實驗數目，減低重建時數值運算之困難，以及增加重建結果之準確性。

第四章則敘述四個實驗實例。包含三埠被動互易電路，三埠被動非互易電路以及雙埠主動電路。重建結果與直接散射矩陣量測結果比較，顯示其一致性，重建誤差亦予以討論。

關鍵字-多埠電路, 散射矩陣量測



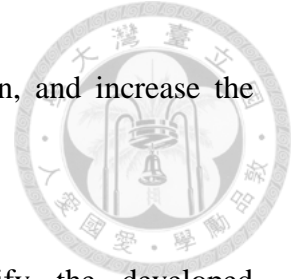
## Abstract

In this dissertation, study results to reconstruct the scattering matrix ( $S$ -matrix) of a multiport network from a set of one-port scattering parameter ( $S$ -parameter) measurements are presented. Port reduction method (PRM) is a method to acquire the  $S$ -matrix of an  $n$ -port network by using a reduced port vector network analyzer (VNA). PRMs have shown that the minimum number of port of a VNA is two or three. This study attempts to go one step further to reduce the number of port to be one, which is the lowest number.

In Chapter 2, reconstruction method using auxiliary circuits and one-port terminations to solve the  $S$ -matrix of a two-port network is described. The type-II PRM is then applied to the results for the reconstruction of the  $S$ -matrix of an  $n$ -port network. Since the terminations used in one-port measurement may cause an active network oscillation. Further development on reconstructing a two-port active network is given. Finally, the method in reconstructing the  $S$ -matrix of a multiport reciprocal network without using PRM is also presented.

The use of auxiliary circuits plays an important role in reducing the number of measured port to be one. The effects of the auxiliary circuits are discussed in Chapter 3. By properly selecting the auxiliary circuit, one can reduce the number of one-port

measurements, ease the problem encountered in the reconstruction, and increase the accuracy of the reconstructed results.



Chapter 4 presents four experimental examples to verify the developed reconstruction methods. They include a three-port reciprocal network, a passive nonreciprocal network and a two-port active network. The reconstructed results are compared with the directly measured  $S$ -matrices. They are shown in good agreement. Errors of reconstructed results are also discussed.

keywords: Multiport network, scattering matrix measurement

# Contents



摘要 .....	i
<b>Abstract</b> .....	<b>ii</b>
<b>Contents</b> .....	<b>iv</b>
<b>Chapter 1 Introduction</b> .....	<b>1</b>
1.1 Multiport network $S$ -matrix measurement .....	1
1.2 Reconstruction methods .....	2
1.3 Port reduction methods .....	2
1.4 Motivation and contribution .....	3
1.5 Chapter outline .....	5
<b>Chapter 2 Formulation</b> .....	<b>10</b>
2.1 Two-port network .....	10
2.1.1 Diagonal elements .....	10
2.1.2 Off-diagonal elements .....	12
2.2 Two-port active network .....	14
2.3 Reciprocal network using comparison process .....	16





2.3.1 Formulation.....	17
2.3.2 Three-port case .....	18
2.4 Summary .....	22
<b>Chapter 3 Selection of auxiliary circuit .....</b>	<b>26</b>
3.1 Two-port network.....	26
3.2 Two-port active network.....	28
3.3 Two-port reciprocal network.....	29
3.4 Summary .....	31
<b>Chapter 4 Experimental results.....</b>	<b>33</b>
4.1 Three-port reciprocal network.....	33
4.2 Three-port nonreciprocal network .....	38
4.3 Two-port active network.....	39
4.4 Three-port reciprocal network using comparison process .....	41
4.5 Summary .....	42
<b>Chapter 5 Conclusion .....</b>	<b>71</b>
<b>Appendices.....</b>	<b>73</b>

Appendix A Prove of $q / p = -(S_{12} + S_{21})$ .....	73
Appendix B Prove of $r / p = S_{12}S_{21}$ .....	73
<b>References</b> .....	<b>74</b>



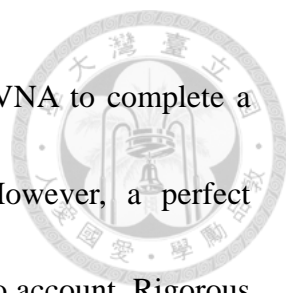
# Chapter 1 Introduction



## 1.1 Multiport network scattering matrix measurement

The scattering matrix ( $S$ -matrix) of a multiport network can be acquired from the direct measurement using a full port vector network analyzer (VNA), or from multiple measurements with the use of a reduced port VNA and proper reconstruction methods [1]-[9]. The former is a straight forward approach. However, the necessary multiport VNA is usually costly and requires complicated calibration [10]-[12] due to the large number of error terms and error paths [11]. In some situations, the multiport calibration can be simplified by ignoring the leakage between each port [13]. As for the situation of non-negligible leakage such as the on-wafer MMIC multiport measurement, Ferrero and Sanpietro proposed a calibration method [14] to take these leakages into account. In [14], one needs to perform 5 calibration steps to obtain 35 linear equations to solve all the error terms of a leaky three-port VNA.

The alternative approach to obtain the  $S$ -matrix of a multiport device-under-test (DUT) is to use a reduced port VNA and certain known terminations. It can characterize a multiport network with less expensive equipments and ease the consideration of calibration. However, the accuracy of results using these approaches would be affected by the numerical issue of the reconstruction algorithm [5], [8], [15], the numerous reconnections during the measurement and the confidence in those known terminations.



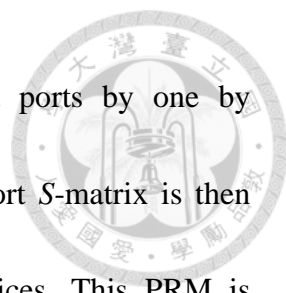
Ideally, one can use perfect terminations and a reduced port VNA to complete a multiport measurement based on the definition of  $S$ -matrix. However, a perfect termination is impractical and the imperfect effect must be taken into account. Rigorous works of this issue have been proposed for decades. These methods using reduced port VNA can be categorized into two types, which are direct reconstruction methods and port reduction methods (PRMs). They will be discussed in the following two sections.

## 1.2 Reconstruction methods

Since a multiport VNA was not as commercially available in early days, some rigorous works [2]-[5] proposed approaches to obtain the  $S$ -matrix of a multiport DUT using a two-port VNA. These approaches have led to build a four-port measurement system using a two-port VNA and switches [6]. The formula of these approaches to reconstruct the  $S$ -matrix of a multiport DUT is based on matrices manipulation. Associated researches in easing the requirement of known terminations [16] and in accuracy analyzing [15] have also been presented. The concept of condition number is used in [15]-[16] to explain how the terminations and the DUT affect the accuracy of results. Such accuracy analysis is complicated and difficult because the matrix manipulation used in these direct reconstruction methods are inherently abstract.

## 1.3 Port reduction methods

On the other hand, [7] provides a different point-of-view in reconstructing an



n-port  $S$ -matrix. This method reduces the number of measured ports by one by connecting a known termination to the unmeasured port. The n-port  $S$ -matrix is then reconstructed from a set of reduced (n-1)-port measured  $S$ -matrices. This PRM is continued until it fails or reaches a port order at which a VNA is available. Three types of PRMs are proposed in [8]-[9]. Reducing one port at a time simplifies the reconstruction problem. The accuracy issue is therefore simpler [8] than that of direct reconstruction methods and can be discussed in a physical sense.

## 1.4 Motivation and contribution

Among the reduced port methods, the reconstruction methods in [1]-[5] can reduce the number of measured ports to two ports. Take the method presented in [5] as an example. The reconstructed n-port  $S$ -matrix can be calculated from (10) in [5] given as

$$S = \Gamma^{-1} - \Sigma^{-1} \quad (1.1)$$

where  $\Gamma$  is an n-by-n diagonal matrix which the diagonal elements are the reflection coefficients of the known terminations. The temporary matrix  $\Sigma$  is calculated from the reflection coefficients of the known terminations and the reduced port measured data.

The measured ports of the reduced port measurement determine which elements in  $\Sigma$  can be calculated as shown in Fig. 1.1. The calculated elements in  $\Sigma$  are always symmetric to the diagonal line. Therefore, the off-diagonal elements will not be calculated if only one-port measurement is performed.



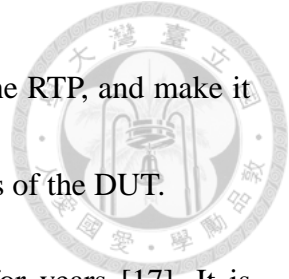
On the other hand, (5) and (6) in [8] given as

$$\left(\frac{1}{\Gamma_{n_1}} - \frac{1}{\Gamma_{n_2}}\right) S_{ij} + (S_{ij}^{(n_1)} - S_{ij}^{(n_2)}) S_{nn} = \frac{S_{ij}^{(n_1)}}{\Gamma_{n_1}} - \frac{S_{ij}^{(n_2)}}{\Gamma_{n_2}} \quad (1.2)$$

$$\left(\frac{1}{\Gamma_{n_1}} - \frac{1}{\Gamma_{n_3}}\right) S_{ij} + (S_{ij}^{(n_1)} - S_{ij}^{(n_3)}) S_{nn} = \frac{S_{ij}^{(n_1)}}{\Gamma_{n_1}} - \frac{S_{ij}^{(n_3)}}{\Gamma_{n_3}} \quad (1.3)$$

imply that the VNA used in applying the type-I PRM should have at least two ports to obtain  $S_{ij}^{(n)}$ . Otherwise, only the diagonal elements of the  $S$ -matrix of the DUT can be solved. Similar restriction can be observed in the type-II PRM [8]. The VNA must have at least two ports to get the measured data  $S_{in}^{(n-1)}$  which appears in (16) of [8]. As for the type-III PRM, the condition  $i \neq j$  stated in (8) of [9] clearly points that the type-III PRM is not suitable for one-port VNA. In fact, the type-III PRM could reduce the number of measured ports to two ports for reciprocal circuits or three ports for nonreciprocal circuits.

Conventionally, it is believed that the reconstruction by reducing the measured ports to one port is quite difficult because the forward transmission coefficient always multiplies with the backward transmission coefficient in a round trip path (RTP) to be defined later. Fig 1.2 illustrates the problem in reducing the minimum number of measured port to be one by using (n-1) one-port terminations. To solve this problem, an auxiliary circuit is proposed in this study to provide additional signal paths as shown in Fig 1.3 by taking a two-port DUT as an example. Such an arrangement will give the



one-port measured data of the VNA contains more information of the RTP, and make it possible to separate the forward and reverse transmission coefficients of the DUT.

One-port VNA or six-port reflectometer has been available for years [17]. It is much simpler in operation and less expensive than two-port and multiport VNAs. The use of one-port VNAs can perform measurements of the insertion loss and the distance to the fault of a cable and the reflection coefficient of a one-port DUT. Recently, USB based one-port VNAs, such as Anritsu MS46121A and Copper Mountain Technologies R54, are available. These then lead to this study of reducing the measured ports of a multiport DUT to the minimum number to be one and acquiring its multiport  $S$ -matrix in a cost-effective manner. Extending the operating frequency to the THz range, one-port VNA can further ease the implementation difficulty of a sub-mmw multiport VNA.

## **1.5 Chapter outline**

Since the reduced port methods [1]-[9] can be applied to reduce the measured ports to two ports, Chapter 2 mainly describes the formulation of acquiring the  $S$ -matrix of a two-port DUT from one-port measurements with the use of an auxiliary circuit. The formulation in dealing with the two-port DUT, including reciprocal and nonreciprocal, is presented in Section. 2.1. The modified formulation for a two-port active network is described in Section 2.2. Section 2.3 then describes an alternative method to determine

the  $S$ -matrix of a reciprocal DUT through a comparison process. By using this process, one can characterize an  $n$ -port reciprocal DUT without using the reduced port methods [1]-[9].

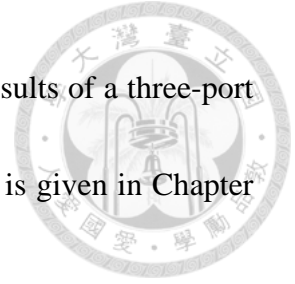


Chapter 3 describes the selection of auxiliary circuit. To reconstruct the  $S$ -matrix of a two-port DUT, the number of one-port measurements in this study is five, which is in excess of that of unknowns by one. However, for certain two-port nonreciprocal networks such as isolator or amplifier as described in Section 3.1, one can properly select the auxiliary circuit to reduce the number of measurements to four to be equal to the number of unknowns. Section 3.2 then gives the criteria of auxiliary circuit in characterizing a two-port active DUT. The effect of the selection of the auxiliary circuit on the accuracy of the reconstructed results is discussed in Section 3.3 for a two-port reciprocal DUT.

Chapter 4 presents four experimental results of reciprocal and nonreciprocal DUTs. Three-port reciprocal and nonreciprocal examples are given in Section 4.1 and Section 4.2, respectively. In each example, the type-II PRM [8] is applied to reconstruct the three-port  $S$ -matrix from two-port results. The reconstruction of two-port  $S$ -matrix from one-port measurements is performed using the formulation to be presented in Section 2.1. The reason to use the type-II PRM rather than the type-I [8] or the type-III PRM [9] is based on the fact that fewer one-port measurements are involved. Section 4.3 shows



the results of a two-port active DUT, while Section 4.4 shows the results of a three-port reciprocal DUT by using comparison process. Finally, a conclusion is given in Chapter 5.



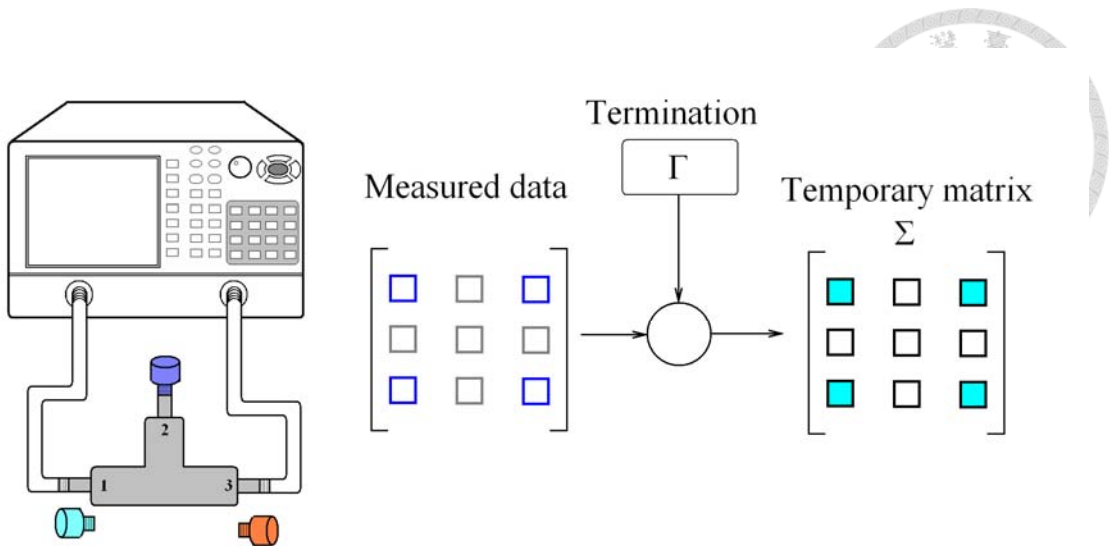


Fig 1.1 Illustration of the elements in  $\Sigma$  and the measured ports of the reduced port measurement.

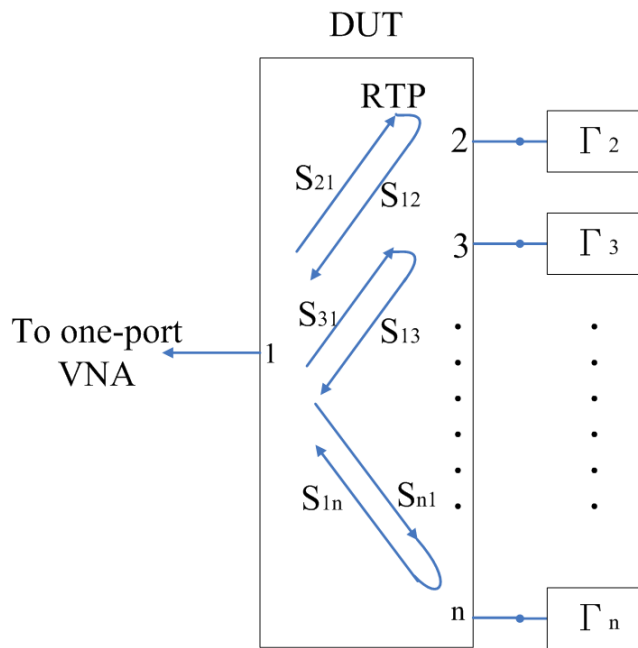


Fig 1.2 Signal flows in one-port measurement using (n-1) one-port terminations.

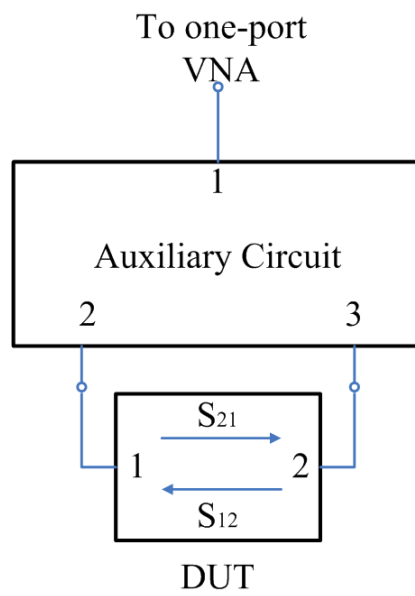
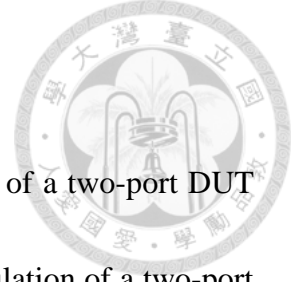


Fig 1.3 Assembly of auxiliary circuit and DUT.

## Chapter 2 Formulation



This chapter describes the formulation of solving the  $S$ -matrix of a two-port DUT from a set of one-port measurements. Section 2.1 presents the formulation of a two-port DUT. Section 2.2 then modifies the formulation to the case of a two-port active DUT. One can then apply PRMs to the two-port results to reconstruct the  $S$ -matrix of an  $n$ -port DUT. In Section 2.3, by applying the symmetry property of a reciprocal DUT, one can find the  $S$ -matrix of an  $n$ -port reciprocal DUT through a comparison process [18] without using the reduced port methods [1]-[9].

### 2.1 Two-port network

In this section, the formulation of solving the diagonal elements of a two-port  $S$ -matrix from one-port measurements is given in Section 2.1.1. The formulation of solving the off-diagonal elements with the use of auxiliary circuits is then given in Section 2.1.2.

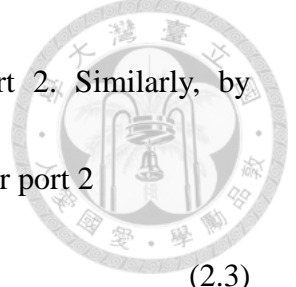
#### 2.1.1 Diagonal elements

The reflection coefficient at port 1 of a two-port DUT by terminating its port 2 with  $\Gamma_2$  is given by

$$S_{11}^{(2)} = S_{11} + \frac{S_{12}S_{21}\Gamma_2}{1 - S_{22}\Gamma_2} \quad (2.1)$$

or

$$S_{11} + S_{11}^{(2)}\Gamma_2 S_{22} + \Gamma_2 (S_{12}S_{21} - S_{11}S_{22}) = S_{11}^{(2)}. \quad (2.2)$$



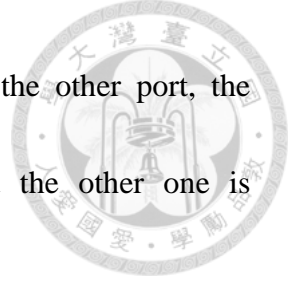
The superscript of  $S_{11}^{(2)}$  denotes that the terminated port is port 2. Similarly, by terminating port 1 with  $\Gamma_1$ , one can obtain the following equation for port 2

$$S_{22} + S_{22}^{(1)}\Gamma_1 S_{11} + \Gamma_1(S_{12}S_{21} - S_{11}S_{22}) = S_{22}^{(1)}. \quad (2.3)$$

From (2.2) and (2.3), one may find that with the help of three known terminations, for example,  $\Gamma_{2a}$ ,  $\Gamma_{2b}$ , and  $\Gamma_{1a}$ , the three unknowns of  $S_{11}$ ,  $S_{22}$  and  $S_{12}S_{21} - S_{11}S_{22}$  could be solved. After that, one can obtain  $S_{12}S_{21}$  by substituting the solved  $S_{11}$  and  $S_{22}$  into (2.2) or (2.3). Therefore, from three one-port measurements of a two-port DUT by terminating the other port with three different known terminations, one can solve the diagonal elements  $S_{11}$  and  $S_{22}$  and the *RTP* term  $S_{12}S_{21} \equiv RTP$  through the following matrix equation

$$\begin{bmatrix} 1 & S_{11}^{(2a)}\Gamma_{2a} & \Gamma_{2a} \\ 1 & S_{11}^{(2b)}\Gamma_{2b} & \Gamma_{2b} \\ S_{22}^{(1a)}\Gamma_{1a} & 1 & \Gamma_{1a} \end{bmatrix} \begin{bmatrix} S_{11} \\ S_{22} \\ RTP - S_{11}S_{22} \end{bmatrix} = \begin{bmatrix} S_{11}^{(2a)} \\ S_{11}^{(2b)} \\ S_{22}^{(1a)} \end{bmatrix}. \quad (2.4)$$

In the above procedure, one sequentially connects two terminations at port 2 and one termination at port 1 of DUT to solve the diagonal elements. Note, the diagonal elements can also be solved if all the three terminations are sequentially connected at port 1 or port 2. However, (2.4) is recommended for the consideration of accuracy. Considering (2.1), corresponding to the case of connecting  $\Gamma_2$  at port 2,  $S_{11}$  is an individual unknown term while  $S_{22}$  is embedded in the denominator. The sensitivities of solving  $S_{11}$  and  $S_{22}$  are different. Further experimental results indicate that by



connecting one termination at one port and two terminations at the other port, the accuracy of one diagonal element becomes slightly worse and the other one is dramatically improved.

Note the *RTP* term in (2.4) is a multiplication of the forward transmission coefficient  $S_{21}$  and the reverse transmission coefficient  $S_{12}$ . Hence, the separation of  $S_{21}$  and  $S_{12}$  needs additional measurements using an auxiliary circuit to be discussed in Section 2.1.2.

### 2.1.2 Off-diagonal elements

In Fig. 1.3, a three-port auxiliary circuit is used to separate the *RTP* term in (2.4). The three ports of the auxiliary circuit are denoted as  $P_1$ ,  $P_2$  and  $P_3$ . Its  $S$ -matrix is known and given by  $\mathbf{A}$  whose elements are  $a_{ij}$  with  $i, j=1, 2, 3$ . Note that the auxiliary circuit needs advance characterization using a three-port VNA.

As shown in Fig. 1.3, port  $P_1$  is connected to a VNA for one-port measurement. Ports 1 and 2 of the DUT are connected to ports  $P_2$  and  $P_3$  of the auxiliary circuit. The measured reflection coefficient  $\Gamma_m$  at port  $P_1$  is given as [5]

$$\Gamma_m = \mathbf{A}_{11} + \mathbf{A}_{12} \mathbf{S} [\mathbf{I} - \mathbf{A}_{22} \mathbf{S}]^{-1} \mathbf{A}_{12} . \quad (2.5)$$

In (2.5)  $\mathbf{S}$  is a two-port  $S$ -matrix of the DUT,  $\mathbf{I}$  is a unit matrix, and the remaining matrices related to the auxiliary circuit are given by



$$\mathbf{A} = \begin{bmatrix} \mathbf{A}_{II} & \mathbf{A}_{IJ} \\ \mathbf{A}_{JI} & \mathbf{A}_{JJ} \end{bmatrix} = \begin{bmatrix} a_{11} & a_{12} & a_{13} \\ a_{21} & a_{22} & a_{23} \\ a_{31} & a_{32} & a_{33} \end{bmatrix}. \quad (2.6)$$

By substituting (2.6) into (2.5), it can be explicitly expressed as

$$\Gamma_m - a_{11} = \frac{N_0 + N_1 S_{12} + N_2 S_{21}}{D_0 + D_1 S_{12} + D_2 S_{21}} \equiv B \quad (2.7)$$

where

$$\begin{aligned} N_0 &= a_{12}a_{21}S_{11} + a_{13}a_{31}S_{22} \\ &\quad + (a_{12}a_{23}a_{31} + a_{13}a_{32}a_{21} - a_{12}a_{21}a_{33} - a_{13}a_{31}a_{22})S_{11}S_{22} \\ &\quad + (a_{12}a_{21}a_{33} + a_{13}a_{31}a_{22} - a_{12}a_{31}a_{23} - a_{13}a_{32}a_{21})S_{12}S_{21} \\ N_1 &= a_{12}a_{31} \\ N_2 &= a_{13}a_{21} \end{aligned} \quad (2.8)$$

and

$$\begin{aligned} D_0 &= 1 - a_{22}S_{11} - a_{33}S_{22} + (a_{22}a_{33} - a_{23}a_{32})S_{11}S_{22} \\ &\quad + (a_{23}a_{32} - a_{22}a_{33})S_{12}S_{21} \\ D_1 &= -a_{32} \\ D_2 &= -a_{23}. \end{aligned} \quad (2.9)$$

One can further express  $S_{12}$  as

$$S_{12} = \frac{RTP}{S_{21}} \quad (2.10)$$

and rewrite (2.7) as a quadratic equation of  $S_{21}$  given by

$$(N_2 - BD_2)S_{21}^2 + (N_0 - BD_0)S_{21} + (N_1 - BD_1)RTP = 0. \quad (2.11)$$

As the auxiliary circuit is properly characterized, all  $a_{ij}$  are known. By using the known  $a_{ij}$  and  $S_{11}$ ,  $S_{22}$  and  $RTP$  solved from (2.4), one can then solve  $S_{21}$ .

However, there are two solutions of  $S_{21}$  from (2.11). An additional one-port



measurement with the use of another auxiliary circuit is needed to solve another set of two solutions of  $S_{21}$ . These two sets then have the correct  $S_{21}$  in common. Once the correct  $S_{21}$  is found,  $S_{12}$  can be calculated using (2.10).

In general, there are a total of five one-port measurements involved to reconstruct the  $S$ -matrix of a two-port DUT. Three one-port measurements are used to solve the diagonal elements  $S_{11}$  and  $S_{22}$  and  $RTP$  term as described in Section 2.1.1. In Section 2.1.2, two additional one-port measurements are performed with the use of two auxiliary circuits to solve the off-diagonal elements  $S_{21}$  and  $S_{12}$ .

For a reciprocal two-port DUT, by applying  $S_{12} = S_{21}$  in (2.7), it becomes a linear equation given by

$$\Gamma_m - a_{11} = \frac{N_0 + (N_1 + N_2)S_{21}}{D_0 + (D_1 + D_2)S_{21}} \quad (2.12)$$

to solve  $S_{21}$  accordingly. Therefore, four one-port measurements are sufficient to reconstruct the  $S$ -matrix of a reciprocal two-port DUT.

Note that for a reciprocal two-port DUT (2.10) can be written as

$$S_{21}^2 = RTP. \quad (2.13)$$

The square root of  $RTP$  gives the sign ambiguity of  $S_{21}$  as discussed in [18], however, (2.12) can solve  $S_{21}$  directly.

## 2.2 Two-port active network

In Section 2.1.1, a one-port termination is connected on the unmeasured DUT port





to solve the diagonal terms. This connection may cause possible oscillation or damage the DUT as the two-port DUT is active. An alternative approach is then developed without using one-port terminations. Instead, five auxiliary circuits are used to perform five one-port measurements.

Since three one-port terminations in Section 2.1 are not used, the diagonal elements become unknowns. Rewrite  $N_0$  in (2.8) as

$$N_0 = N_a S_{11} + N_b S_{22} + N_c (S_{11} S_{22} - S_{12} S_{21}) \quad (2.14)$$

where

$$\begin{aligned} N_a &= a_{12} a_{21} \\ N_b &= a_{13} a_{31} \\ N_c &= a_{12} a_{23} a_{31} + a_{13} a_{32} a_{21} - a_{12} a_{21} a_{33} - a_{13} a_{31} a_{22}. \end{aligned} \quad (2.15)$$

Similarly,  $D_0$  in (2.9) is rewritten as

$$D_0 = 1 + D_a S_{11} + D_b S_{22} + D_c (S_{11} S_{22} - S_{12} S_{21}) \quad (2.16)$$

where

$$\begin{aligned} D_a &= -a_{22} \\ D_b &= -a_{33} \\ D_c &= a_{22} a_{33} - a_{23} a_{32} \end{aligned} \quad (2.17)$$

By substituting (2.14) and (2.16) into (2.7), one can obtain a linear equation as

$$(N_a - B D_a) S_{11} + (N_b - B D_b) S_{22} + (N_1 - B D_1) S_{12} + (N_2 - B D_2) S_{21} + (N_c - B D_c) S_{\det} = B \quad (2.18)$$

where

$$S_{\det} = S_{11} S_{22} - S_{12} S_{21}. \quad (2.19)$$

Note there are five unknowns,  $S_{11}$ ,  $S_{22}$ ,  $S_{12}$ ,  $S_{21}$ , and  $S_{\det}$ , in (2.18). All the



coefficients and constant term in (2.18) are related to the  $S$ -matrix of auxiliary circuit and measured data. Therefore, one can solve these five unknowns through five one-port measurements with the use of five different auxiliary circuits.

## 2.3 Reciprocal network using comparison process

This section describes a method to obtain the  $S$ -matrix of an  $n$ -port reciprocal DUT without using the reduced port methods [1]-[9]. At first, the diagonal elements of the  $n$ -port  $S$ -matrix and the  $RTP$  terms will be solved. By applying the symmetric property of the  $S$ -matrix of a reciprocal DUT, the off-diagonal elements can then be solved by directly taking square root of the  $RTP$  terms. However, this will result in several possible  $S$ -matrices, and it will encounter an ambiguity problem in selecting the correct one. To solve this, additional one-port measurements are performed with the use of a characterized  $(n-1)$ -port auxiliary circuit. On the other hand, by applying the  $S$ -matrix of the auxiliary circuit and all the possible  $S$ -matrices, one can calculate all the possible one-port measured values according to the assembly of the DUT and the auxiliary circuit. These calculated results are then compared with the one-port measured results. The comparison results will then determine the correct  $S$ -matrix.

The formulation and the concept of solving the  $RTP$  terms and the diagonal elements of the  $S$ -matrix of a reciprocal DUT is described in Section 2.3.1. The method in finding the correct  $S$ -matrix and the way to reduce the number of one-port



measurements is described with a three-port DUT case as shown in Section 2.3.2.

### 2.3.1 Formulation

This section starts with (2.1) and a three-port DUT which its port 3 is terminated with a termination. After the explanation of the notation and the introduction of the formulation, the solution will then extend to an n-port DUT case.

Since a three-port DUT can be regarded as a two-port network if one of its port is terminated, the method in Section 2.1.1 to solve the reflection coefficients and the *RTP* term of a two-port network still stands in this case. However, the terms in (2.1) needs to be modified to show the difference between a two-port DUT and a three-port DUT. The modified equation of (2.1) is given as

$$S_{11}^{(3,2)} = S_{11}^{(3)} + \frac{S_{12}^{(3)} S_{21}^{(3)} \Gamma_2}{1 - S_{22}^{(3)} \Gamma_2} \quad (2.20)$$

The term  $S_{11}^{(3,2)}$  is the reflection coefficient measured at port 1 of the DUT with its port 3 and port 2 are terminated with terminations. The superscript denotes the port or ports that are terminated with known terminations. From (2.20), one can solve  $S_{11}^{(3)}$ ,  $S_{22}^{(3)}$  and  $S_{12}^{(3)} S_{21}^{(3)}$  with the use of three terminations  $\Gamma_{2a}$ ,  $\Gamma_{2b}$ , and  $\Gamma_{2c}$ . After that, since the intermediate parameter  $S_{11}^{(3)}$  is composed as

$$S_{11}^{(3)} = S_{11} + \frac{S_{13} S_{31} \Gamma_3}{1 - S_{33} \Gamma_3}, \quad (2.21)$$

the reflection coefficients and the *RTP* term of the three-port DUT, e.g.  $S_{11}$ ,  $S_{33}$ , and



$S_{13}S_{31}$ , can be solved with the use of three terminations  $\Gamma_{3a}$ ,  $\Gamma_{3b}$ , and  $\Gamma_{3c}$ .

The above procedure shows two things that should be noticed. The first is that the intermediate *RTP* terms such as  $S_{12}^{(3)}S_{21}^{(3)}$  are helpless in solving the *S*-parameters of the next higher order in port number. The other is that the number of measurements to solve the diagonal elements of an *n*-port DUT is theoretically  $3^{(n-1)}$ .

To extend to an *n*-port DUT, (2.20) can be rewritten as

$$S_{11}^{(n,n-1,\dots,3,2)} = S_{11}^{(n,n-1,\dots,3)} + \frac{S_{12}^{(n,n-1,\dots,3)} S_{21}^{(n,n-1,\dots,3)} \Gamma_2}{1 - S_{22}^{(n,n-1,\dots,3)} \Gamma_2}. \quad (2.22)$$

From (2.22), it is clear that with three terminations placed in sequence, one can find some of the intermediate parameters of the higher order in port number. A general form of (2.22) is shown below, which could help finding the arbitrary intermediate parameters. It is given as

$$S_{ii}^{(n,n-1,\dots,k+1,k,k-1,\dots)} = S_{ii}^{(n,n-1,\dots,k+1,k-1,\dots)} + \frac{S_{ik}^{(n,n-1,\dots,k+1,k-1,\dots)} S_{ki}^{(n,n-1,\dots,k+1,k-1,\dots)} \Gamma_k}{1 - S_{kk}^{(n,n-1,\dots,k+1,k-1,\dots)} \Gamma_k}. \quad (2.23)$$

### 2.3.2 Three-port case

Section 2.3.1 has described the method in finding the *RTP* terms and the diagonal elements of the *S*-matrix of an *n*-port reciprocal DUT. This section will use a three-port reciprocal DUT as a specific example to demonstrate how to find the off-diagonal elements. Furthermore, by properly choosing the terminated port of the DUT and arranging the one-port measurements, the number of one-port measurements can be



reduced to be less than  $3^{(n-1)}$ .

At first, a generalized form of (2.1) can be expressed as

$$S_{ii}^{(j)} = S_{ii} + \frac{S_{ij}S_{ji}\Gamma_j}{1 - S_{jj}\Gamma_j}. \quad (2.24)$$

Consider a three-port reciprocal DUT with its port 3 is terminated with  $\Gamma_{3a}$ , (2.20) can be rewritten as

$$S_{11}^{(3a,2)} = S_{11}^{(3a)} + \frac{S_{12}^{(3a)}S_{21}^{(3a)}\Gamma_2}{1 - S_{22}^{(3a)}\Gamma_2} \quad (2.25)$$

and (2.4) becomes

$$\begin{bmatrix} 1 & S_{11}^{(3a,2a)}\Gamma_{2a} & \Gamma_{2a} \\ 1 & S_{11}^{(3a,2b)}\Gamma_{2b} & \Gamma_{2b} \\ S_{22}^{(3a,1a)}\Gamma_{1a} & 1 & \Gamma_{1a} \end{bmatrix} \begin{bmatrix} S_{11}^{(3a)} \\ S_{22}^{(3a)} \\ S_{12}^{(3a)}S_{21}^{(3a)} - S_{11}^{(3a)}S_{22}^{(3a)} \end{bmatrix} = \begin{bmatrix} S_{11}^{(3a,2a)} \\ S_{11}^{(3a,2b)} \\ S_{22}^{(3a,1a)} \end{bmatrix}. \quad (2.26)$$

With the help of (2.26), one can solve the two intermediate parameters  $S_{11}^{(3a)}$  and  $S_{22}^{(3a)}$ .

Another two intermediate parameters  $S_{11}^{(3b)}$  and  $S_{22}^{(3b)}$  can also be solved from (2.26)

by simply replacing  $\Gamma_{3a}$  with  $\Gamma_{3b}$ . Similarly, the last two parameters  $S_{22}^{(1a)}$  and

$S_{33}^{(1a)}$  could be solved by terminating the port 1 of a three-port DUT with  $\Gamma_{1a}$ . The

necessary one-port measurements are summarized in Table 2.1 (a). In this table the

corresponding one-port measurement of  $S_{11}^{(3a,2a)}$ , for example, is denoted as “1\_3a2a”.

The notation “\*” marks the repeated measurement.



As described in Table 2.1 (a), six intermediate parameters are solved accordingly.

One can then use these intermediate parameters to find all the possible  $S$ -parameters of the three-port DUT in the following three steps.

In the first step, one may solve  $S_{11}$  and  $S_{33}$  by replacing all the 2's in (2.4) with 3's based on the three intermediate parameters of  $S_{11}^{(3a)}$ ,  $S_{11}^{(3b)}$  and  $S_{33}^{(1a)}$ . In addition, one can also obtain  $S_{13}S_{31}$  by substituting  $S_{11}$  and  $S_{33}$  into the expression of  $S_{13}S_{31} - S_{11}S_{33}$ . Therefore, in this step,  $S_{11}$ ,  $S_{33}$  and  $S_{13}S_{31}$  are solved as illustrated in the first row of Table 2.1 (b).

In the second step, one can use the intermediate parameters  $S_{22}^{(3a)}$  and  $S_{22}^{(3b)}$  with the case  $(i, j) = (2, 3)$  in (2.24) to write the corresponding matrix equation. Since  $S_{33}$  is solved already, one can solve the unknowns of  $S_{22}$  and  $S_{23}S_{32}$  using (2.27) as illustrated in the second row of Table 2.1 (b).

$$\begin{bmatrix} 1 & \Gamma_{3a} \\ 1 & \Gamma_{3b} \end{bmatrix} \begin{bmatrix} S_{22} \\ S_{23}S_{32} \end{bmatrix} = \begin{bmatrix} S_{22}^{(3a)} - S_{22}^{(3a)}\Gamma_{3a}S_{33} \\ S_{22}^{(3b)} - S_{22}^{(3b)}\Gamma_{3a}S_{33} \end{bmatrix}. \quad (2.27)$$

In the last step, one can then calculate  $S_{12}S_{21}$  by using the intermediate parameter  $S_{22}^{(1a)}$  with (2.24) as

$$\frac{(S_{22}^{(1a)} - S_{22})(1 - S_{11}\Gamma_{1a})}{\Gamma_{1a}} = S_{12}S_{21} \quad (2.28)$$

in which  $S_{11}$  and  $S_{22}$  are already solved. This step is illustrated in the third row of Table 2.1 (b).




Table 2.1 (b) then summarizes the procedures given above. The notation “\*\*” marks the parameters already solved in the second step. The solved results in Table 2.1 (b) include the three diagonal elements. As for the off-diagonal elements, because the three-port DUT is reciprocal, one can simply take the square root of the solved results of  $S_{12}S_{21}$ ,  $S_{13}S_{31}$  and  $S_{23}S_{32}$ . However, this would yield two possible values which are  $180^\circ$  apart for each term. If we use “+” and “-” to denote the solution in the upper half and lower half complex plane, there are eight configurations for  $(S_{12}, S_{13}, S_{23})$  with ambiguities from (+, +, +) to (-, -, -).

To separate the off-diagonal  $S$ -parameters apart, one needs additional one-port measurement as shown in Fig. 2.1. According to the assembly in Fig. 2.1(a), the DUT port 2 and port 3 are connected to a known two-port auxiliary circuit. It then may give signal paths not containing the RTP. Such paths can then be used to avoid the self multiplication terms.

To achieve this, all the eight configurations are firstly listed, then the  $S$ -matrix of the auxiliary circuit is applied to calculate the eight reflection coefficients according to the arrangement of Fig 2.1 (a). Experimental study to be presented in Section 4.4 for an Agilent 11667B power splitter is used as a three-port reciprocal DUT. By comparing the calculated and measured reflection coefficients, there are six configurations showing the inconsistency as illustrated in Fig. 2.2. The vertical axis of Fig. 2.2 shows the distance

of the measured and calculated reflection coefficients defined as

$$Distance = |\Gamma_{Calculated} - \Gamma_{Measured}| \quad (2.29)$$



where “ $\Gamma$ ” denotes the reflection coefficient. As for the remainder 2 configurations of (+, +, -) and (-, -, -), another one-port measurement as shown in Fig 2.1 (b) is performed to help selecting the correct one. Reconstructed results will be given in Section 4.4.

## 2.4 Summary

The formulations in reconstructing the  $S$ -matrix of a two-port network or an  $n$ -port reciprocal network are presented in this chapter. To reduce the possibility of damaging the DUT, the experimental procedure and the formulations for active devices are modified. Generally speaking, the auxiliary circuits are required to be fully known. However, the requirement of the auxiliary circuits used in the comparison process given in Section 2.3 can be relaxed. Since the possible off-diagonal elements obtained in the comparison process are  $180^\circ$  apart, a rough knowledge of the auxiliary circuits is sufficient to determine the correct  $S$ -parameters.

Note that reconstruction methods in [8] and [9] use redundant equations to solve the reflection coefficients of certain terminations. This then leads the terminations can be partially unknown. However, in the one-port measurement case presented in this chapter, only one equation is available in each one-port measurement. It is then difficult



to have redundant equations to make the auxiliary circuit partially known.



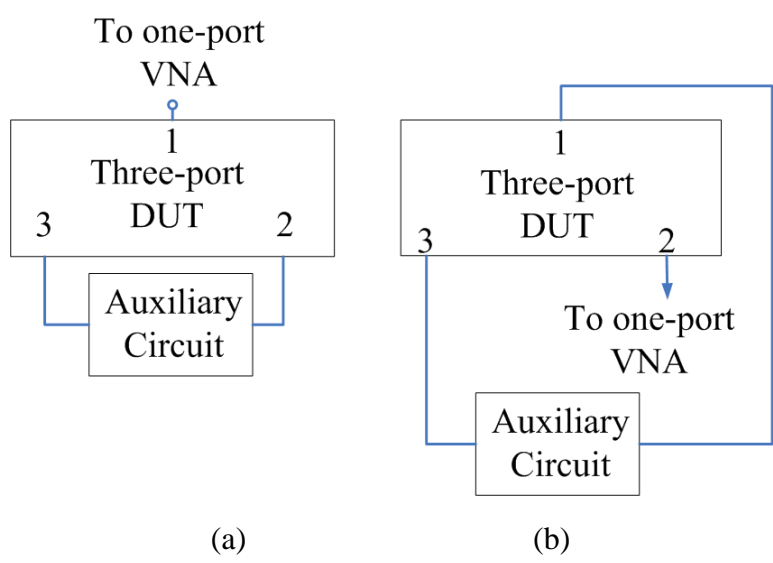


Fig. 2.1 Two arrangements of auxiliary circuit for additional one-port measurements.

Intermediate Parameters	One-Port Measurements	Solved Results	Intermediate Parameters
$S_{11}^{(3a)}$ $S_{22}^{(3a)}$	1_3a2a	$S_{11}$ $S_{33}$ $S_{13}S_{31}$	$S_{11}^{(3a)}$
	1_3a2b		$S_{11}^{(3b)}$
	2_3a1a		$S_{33}^{(1a)}$
$S_{11}^{(3b)}$ $S_{22}^{(3b)}$	1_3b2a	$S_{22}$ $S_{23}S_{32}$	$S_{22}^{(3a)}$
	1_3b2b		$S_{22}^{(3b)}$
	2_3b1a		$S_{33}^{**}$
$S_{22}^{(1a)}$ $S_{33}^{(1a)}$	2_3a1a *	$S_{12}S_{21}$	$S_{22}^{(1a)}$
	2_3b1a *		$S_{11}^{**}$
	3_2a1a		$S_{22}^{**}$

Table 2.1 (a) The intermediate parameters from one-port measurements and (b) the intermediate parameters for solving the results.

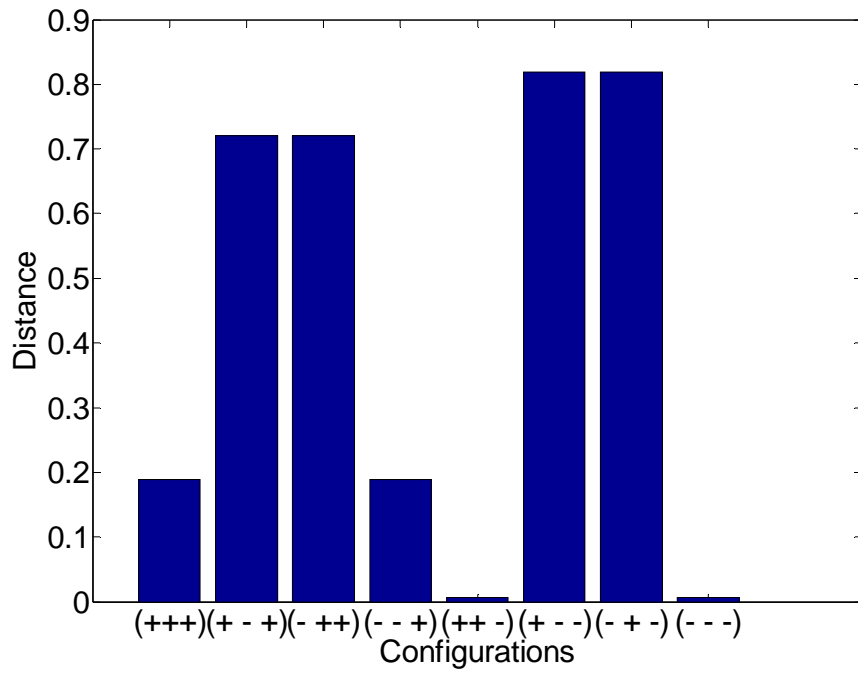
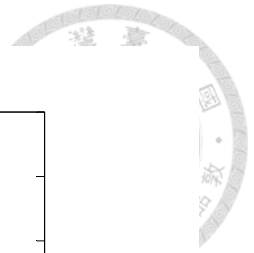


Fig. 2.2 The distance between calculated and measured reflection coefficients at port 1 for eight configurations.

## Chapter 3 Selection of auxiliary circuit



Formulation has been presented in Chapter 2 to reconstruct the  $S$ -matrix of a two-port from a set of one-port measurements using auxiliary circuits. This chapter will discuss the effect of the auxiliary circuit in terms of the three following items, the reduction of the number of one-port measurements, the solvability, and the accuracy of the reconstructed results.

Section 3.1 describes the suggestion in selecting the auxiliary circuit used in the reconstruction method presented in Section 2.1, and the number of one-port measurements can be reduced to four for certain two-port nonreciprocal DUTs. Section 3.2 then describes the criteria of the auxiliary circuits for a two-port active network. Finally, to increase the accuracy of the reconstructed result for a reciprocal DUT in Section 2.1, Section 3.3 discusses the consideration of the auxiliary circuit.

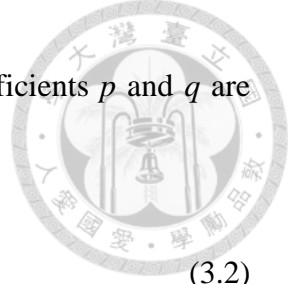
### 3.1 Two-port network

In this section, the effect of auxiliary circuit on the roots of (2.11) is discussed. The possibility to reduce the number of one-port measurements to four for certain two-port nonreciprocal DUT is also addressed.

Note (2.11) can be rewritten in a simpler quadratic form as

$$pS_{21}^2 + qS_{21} + r = 0 \quad (3.1)$$

where  $p$ ,  $q$  and  $r$  represent the corresponding coefficients. It will be proved in Appendix



As that for a three-port reciprocal auxiliary circuit, the ratio of coefficients  $p$  and  $q$  are given as

$$\frac{q}{p} = -(S_{12} + S_{21}). \quad (3.2)$$

The coefficients of  $p$  and  $r$  are further related by

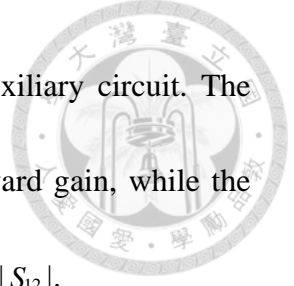
$$\frac{r}{p} = S_{12}S_{21}. \quad (3.3)$$

as proved in Appendix B.

According to Vieta's formulas for quadratics [19], from (3.2) and (3.3), the two roots of (2.11) must be  $S_{12}$  and  $S_{21}$  if the three-port auxiliary circuit is reciprocal. On the contrary, for a nonreciprocal auxiliary circuit, only one of the two roots is  $S_{21}$ , while the other is meaningless.

This leads that one should use a reciprocal auxiliary circuit and (2.12) to solve the transmission coefficient of a reciprocal DUT as suggested in row (1) of Table 3.1. Further discussion on using a reciprocal auxiliary circuit for a two-port reciprocal DUT will be given in the Section 3.3 based on the accuracy consideration.

For certain two-port nonreciprocal DUTs whose  $S_{12}$  and  $S_{21}$  are distinguishable, with the use of one reciprocal auxiliary circuit as suggested in row (2) of Table 3.1, one could easily identify  $S_{21}$  and  $S_{12}$  from the roots of (2.11). The other additional auxiliary circuit as described in Section 2.1.2 to identify the correct  $S_{21}$  is therefore not necessary. The resulting number of one-port measurements is then four.



Amplifier is a typical example to use only one reciprocal auxiliary circuit. The larger root of (2.11) should be  $S_{21}$  representing the amplifier forward gain, while the other is  $S_{12}$ . Isolator is another typical example, because its  $|S_{21}| \gg |S_{12}|$ .

As for a general two-port nonreciprocal DUT, one needs two three-port auxiliary circuits. Note one of the auxiliary circuits should be nonreciprocal as suggested in row (3) of Table 3.1. Otherwise, the two sets of roots will be identical. Table 3.1 summarizes the suggestion on selecting the proper auxiliary circuit for a two-port DUT.

### 3.2 Two-port active network

This section will discuss the solvability of (2.18) for a two-port active DUT in terms of the auxiliary circuit. As described in Section 2.2, one can reconstruct the  $S$ -matrix of a two-port active DUT with five one-port measurements and (2.18). Specifically, the  $S$ -matrix is determined through the following matrix equation

$$\Sigma \mathbf{X} = \mathbf{B} \quad (3.4)$$

where

$$\Sigma = \begin{bmatrix} N_a^{(1)} - BD_a^{(1)} & N_b^{(1)} - BD_b^{(1)} & N_1^{(1)} - BD_1^{(1)} & N_2^{(1)} - BD_2^{(1)} & N_c^{(1)} - BD_c^{(1)} \\ N_a^{(2)} - BD_a^{(2)} & N_b^{(2)} - BD_b^{(2)} & N_1^{(2)} - BD_1^{(2)} & N_2^{(2)} - BD_2^{(2)} & N_c^{(2)} - BD_c^{(2)} \\ \dots & \dots & \dots & \dots & \dots \\ N_a^{(5)} - BD_a^{(5)} & N_b^{(5)} - BD_b^{(5)} & N_1^{(5)} - BD_1^{(5)} & N_2^{(5)} - BD_2^{(5)} & N_c^{(5)} - BD_c^{(5)} \end{bmatrix} \quad (3.5)$$

and

$$\mathbf{X} = \begin{bmatrix} S_{11} \\ S_{22} \\ S_{12} \\ S_{21} \\ S_{\det} \end{bmatrix} \quad \mathbf{B} = \begin{bmatrix} B^{(1)} \\ B^{(2)} \\ B^{(3)} \\ B^{(4)} \\ B^{(5)} \end{bmatrix}. \quad (3.6)$$



Note that the superscripts in (3.5) and (3.6) denote the five one-port measurements. The other superscripts used in the expressions in Chapter 2 denote the terminated port of DUT and the corresponding termination.

By substituting (2.8) and (2.9) into (2.18), the coefficients of  $S_{12}$  and  $S_{21}$  can be represented as

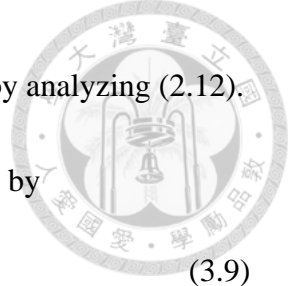
$$N_1 - BD_1 = a_{12}a_{31} + Ba_{32} \quad (3.7)$$

$$N_2 - BD_2 = a_{21}a_{13} + Ba_{23}. \quad (3.8)$$

From (3.7) and (3.8), one can find that if a reciprocal auxiliary circuit is used, the coefficients of  $S_{12}$  and  $S_{21}$  are identical. Therefore, if the five auxiliary circuits used in Section 2.2 are all reciprocal, the third and fourth columns of  $\Sigma$  become the same. As the result, the determinant of  $\Sigma$  is zero and (3.5) is not solvable. This then leads that at least one of the five auxiliary circuits used in Section 2.2 must be nonreciprocal to guarantee the solvability of (3.5). It is also consistent with the suggestion given in Table 3.1.

### 3.3 Two-port reciprocal network

This section will discuss the selection of the auxiliary circuit to improve the



accuracy of the reconstructed results for a two-port reciprocal DUT by analyzing (2.12).

According to (2.12),  $S_{21}$  of a two-port reciprocal DUT is given by

$$S_{21} = \frac{(\Gamma_m - a_{11})D_0 - N_0}{(\Gamma_m - a_{11})(a_{23} + a_{32}) + (a_{12}a_{31} + a_{13}a_{21})}. \quad (3.9)$$

If the magnitude of the denominator of (3.9) is small approaching to zero, the accuracy of  $S_{21}$  will be affected. Specifically, the accuracy of the resulting  $S_{21}$  becomes poor if

$$(\Gamma_m - a_{11})(a_{23} + a_{32}) + (a_{12}a_{31} + a_{13}a_{21}) \cong 0. \quad (3.10)$$

Since port 1 is the port connected to the VNA,  $a_{11}$  determines how much power to the DUT. It is then practical to have the  $a_{11}$  term of the auxiliary circuit to have small value. Based on this assumption, (3.10) indicates that the accuracy will be poor as

$$\Gamma_m \cong \frac{-a_{12}a_{31} - a_{13}a_{21}}{a_{23} + a_{32}} \quad (3.11)$$

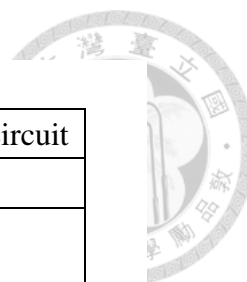
Based on the experimental examples to be presented in Chapter 4, an Agilent 11667B power splitter and a DITOM D3C2040 circulator are used as reciprocal and nonreciprocal three-port auxiliary circuits. The magnitude of the right side term of the  $\cong$  sign in (3.11) is about 30 and 0.88 for Agilent 11667B power splitter and DITOM D3C2040 circulator, respectively. Therefore, one should use a power splitter as the auxiliary circuit for a two-port reciprocal DUT from the accuracy consideration, because the measured value of  $|\Gamma_m|$  is less than 1 being closer to 0.88 to give poor accuracy by using a circulator as the auxiliary circuit. This is also consistent with the suggestion in row (1) of Table 3.1.



### 3.4 Summary

This chapter describes the suggestions in selecting the auxiliary circuit. By proper selecting the auxiliary circuit, the amount of experiments can be reduced. In addition, the unable-solved situations can be avoided and the accuracy of the reconstructed results can be improved. Since the three-port auxiliary circuits must be characterized in advance, further study may be performed to ease the reliance on the three-port auxiliary circuit. For example, one can connect a known two-port circuit to a three-port auxiliary circuit and perform one-port measurements. It might be possible to characterize the auxiliary circuit using the developed reconstruction methods.





	Two-port DUT	Three-port auxiliary circuit
(1)	reciprocal	one reciprocal
(2)	non-reciprocal having distinguishable $S_{21}$ and $S_{12}$	one reciprocal
(3)	general nonreciprocal	at least one nonreciprocal

Table 3.1 Suggestion on the auxiliary circuit.

## Chapter 4 Experimental results



This chapter presents four experimental examples to verify the approaches presented in Chapter 2. By applying the reconstruction method of Section 2.1 and the type-II PRM, the  $S$ -matrices of two three-port DUTs, one for reciprocal case and another for nonreciprocal case, are presented in Section 4.1 and Section 4.2, respectively. Specifically, one uses the method presented in Section 2.1 to reconstruct the intermediate two-port  $S$ -matrices from a set of one-port measurements. The type-II PRM is then used to acquire the three-port  $S$ -matrix from those reconstructed two-port  $S$ -matrices. In addition, the experiment arrangement and the explanation of the notations are also explained in Section 4.1. Section 4.3 demonstrates the reconstruction of a two-port active DUT using the method described in Section 2.2. Finally, the reconstructed results of a three-port reciprocal DUT using comparison process as described in Section 2.3 are shown in Section 4.4.

### 4.1 Three-port reciprocal network

Two three-port DUTs are used to verify the method of Section 2.1. One is an Agilent 11667B power splitter as a three-port reciprocal DUT. The other is a DITOM D3I2040 circulator as a three-port nonreciprocal DUT. The three-port DUT is firstly terminated at one port with three known terminations in sequence as three two-port circuits. The method developed in Section 2.1 is then employed to reconstruct the



$S$ -matrices of these three two-port circuits from one-port measurements. The type-II PRM [8] is then used to reconstruct the  $S$ -matrix of the three-port DUT from the resulted three two-port  $S$ -matrices.

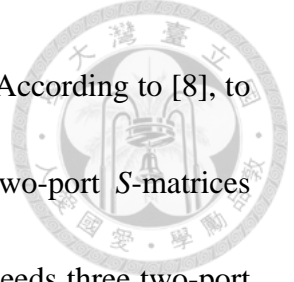
The number of one-port experiments for each two-port circuit is four for Agilent 11667B power splitter because  $S_{12} = S_{21}$ , and (2.12) is sufficient to solve the transmission coefficient. Therefore, an additional Agilent 11667B power splitter is used to be the three-port auxiliary circuit according to Table 3.1 and discussed in Section 3.3.

The one-port measurements of these two experiments are conducted at the port 1 of an Agilent N5222A four-port VNA. The reason to use a four-port VNA to perform one-port measurements is that it will also be used to directly measure the DUT full three-port  $S$ -matrix to verify the reconstructed results. The average error of the reconstructed results is given as

$$100\% \times \frac{1}{N} \sum_{n=1}^N \frac{|S_r(n) - S_m(n)|}{|S_m(n)|} \quad (4.1)$$

where  $S_r$  and  $S_m$  are the reconstructed and directly measured  $S$ -parameters, and  $N$  is the number of frequency points. By comparing the results of using a power splitter and a circulator as the auxiliary circuit in the reciprocal experimental example, using power splitter gives 1.319 % less in average error than using circulator as the auxiliary circuit.

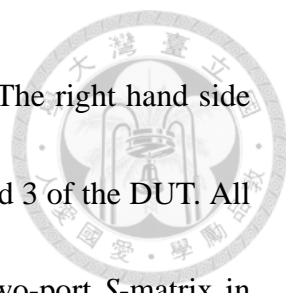
Before the description of experiments, the explanation of using the type-II PRM



rather than the type-I or the type-III PRM is given in the following. According to [8], to reconstruct a three-port  $S$ -matrix, the type-II PRM needs three two-port  $S$ -matrices while the type-I PRM needs four. Although the type-III PRM also needs three two-port  $S$ -matrices, its reconstruction algorithm is more complicated. Furthermore, the type-III PRM cannot deal with a three-port nonreciprocal network because it requires the minimum number of port of a nonreciprocal DUT being four.

Table 4.1 shows the port arrangements for reconstructing the  $S$ -matrix of a three-port DUT from one-port measurements. Each notation in Table 4.1 represents an  $S$ -matrix. It is composed of two parts separated by an underline except for the one in the left column which is a three-port  $S$ -matrix. Note both DUT and auxiliary circuit are involved in the right column for one-port  $S$ -parameters. The left part with number or numbers indicates the port or ports to the corresponding DUT  $S$ -matrix. The left part with  $P_1$  indicates the measured port of auxiliary circuit. The right part describes the known terminations or ports of the auxiliary circuit connected to the rest port or ports of a three-port DUT. The two one-port  $S$ -matrices in the right column marked with \* are duplicated ones.

Taking the first one in the right column for example,  $1\_ \Gamma_{2a} \Gamma_{3a}$  is a one-port  $S$ -parameter for port 1 of a three-port DUT whose ports 2 and 3 are connected to terminations  $\Gamma_{2a}$  and  $\Gamma_{3a}$ . The fourth one in the same column given by  $P_1\_ P_2 \Gamma_{2a} P_3$



is then a one-port  $S$ -parameter for port  $P_1$  of the auxiliary circuit. The right hand side of the underline indicates the elements connected at the ports 1, 2 and 3 of the DUT. All the one-port  $S$ -parameters are obtained from measurements. The two-port  $S$ -matrix in the central column, for example, the first one given by  $13\_ \Gamma_{2a}$ , is reconstructed from four one-port  $S$ -parameters using the described method given in Section 2.1. It is a two-port  $S$ -matrix corresponding to the ports 1 and 3 of DUT with port 2 terminated with  $\Gamma_{2a}$ . Finally, the three-port  $S$ -matrix of DUT in the left column is then reconstructed from the intermediate three two-port  $S$ -matrices using the type-II PRM.

There are a total of twelve one-port  $S$ -parameters as shown in the right column of Table 4.1 to give a total of ten one-port measurements accordingly. The measurement arrangement of the first eight one-port measurements is shown in Fig. 4.1(a) while that of the last two one-port measurements is shown in Fig. 4.1(b). The switches  $S1\sim S3$  are simultaneously toggled. One can either manually connect or disconnect the DUT, auxiliary circuit and terminations or properly use switches  $S1\sim S5$ . According to the positions of switches in Fig. 4.1, the corresponding one-port measurements are  $1\_ \Gamma_{2a}\Gamma_{3b}$  and  $P_1\_ P_2P_3\Gamma_{3a}$ , respectively.

The experiments performed are conducted by manual connections and disconnections. This can avoid the side effects caused by the isolation, loss and mismatch of switches to be discussed in Chapter 5. However, careful operation on



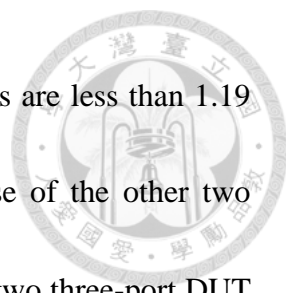
manual connection and disconnection is required. Otherwise, ripples can be found in the reconstructed results.

The details of DUTs, auxiliary circuits and terminations used are listed in Table 4.2.

A short cable and an M-M adapter that are both characterized are used to connect the auxiliary circuit and the DUT. The short cable connects from port  $P_3$  of auxiliary circuit to port 2 or port 3 of DUT, and the adapter connects from port  $P_2$  of auxiliary circuit to port 1 of DUT. The open and short terminations in Table 4.2 are components in Agilent 85052D calibration kit. The 3-, 5- and 6-dB attenuators are HP 8493C, JFW 50HF-005 and JFW 50HF-006, respectively. Fig. 4.2 shows the measurement setup of a nonreciprocal DUT using a reciprocal auxiliary circuit in one-port measurement of  $P_1 - P_2 \Gamma_{2a} P_3$ .

The reciprocal DUT is an Agilent 11667B power splitter as shown in Fig. 4.3(a). Its reconstructed results of magnitude are shown in Fig. 4.4. Directly measured results are also given for comparison. Note the VNA uncertainty is also marked with gray color in the magnitude response and the reconstructed results are shown within the gray region. Fig. 4.5 shows the phase difference of reconstructed and measured results to give a detail examination of the phase variation. The reconstructed  $S$ -parameters are shown in close agreement with those directly measured results from 1 to 5 GHz.

The average errors of  $S$ -parameters are given in Table 4.3 (a). The maximum



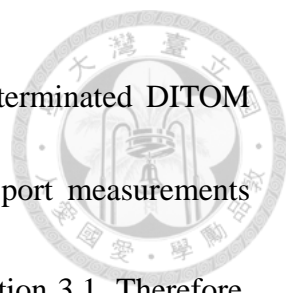
average error is about 5.05 % for  $S_{11}$ , while all other average errors are less than 1.19 %. One can find that the average error of  $S_{11}$  is larger than those of the other two diagonal elements. Similar results can also be observed in the other two three-port DUT examples to be presented later. This can be referred to the following two reasons. The first is the different sensitivity of the solved  $S_{11}$  and  $S_{22}$  in (2.1) as explained in Section 2.1. The second is due to the measurement arrangement as shown in Table 4.1. In order to have the three intermediate circuits given in the central column of Table 4.1 for the use of the type-II PRM, the port 1 of the DUT is mostly connected to the VNA as shown in the right column of Table 4.1 for one-port measurements. This could result that the error of the reconstructed  $S_{11}$  is different from those of  $S_{22}$  and  $S_{33}$ .

The difference of reconstructed results and directly measured results shown in Fig. 4.4 and Fig. 4.5 is mainly caused from the cable-flex repeatability among the one-port measurements. Simulation study using Agilent Advanced Design System (ADS) indicates that small phase deviation of the cable will give errors of reconstructed results in the form of a ripple pattern. Further experiments with the use of two long cables in connecting the auxiliary circuit and the DUT also cause the ripples in the reconstructed results.

## 4.2 Three-port nonreciprocal network

The nonreciprocal DUT is a DITOM D3I2040 circulator as shown in Fig. 4.3(b).

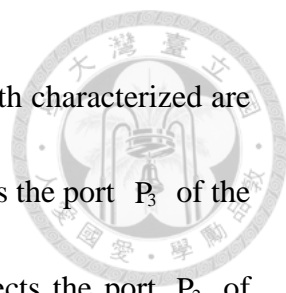




Its operation bandwidth is 2 to 4 GHz. Note because a one-port terminated DITOM D3I2040 circulator has distinguishable  $|S_{12}|$  and  $|S_{21}|$ , four one-port measurements are enough to solve (2.11) according to the discussion given in Section 3.1. Therefore, an Agilent 11667B power splitter is used as the auxiliary circuit for this example. The reconstructed results are shown in Fig. 4.6. The areas filled with light yellow color indicate the regions that outside the operation bandwidth. Note only three  $S$ -parameters are given in Fig. 4.6 and they are the worst cases in reflection coefficient, forward transmission coefficient and reverse transmission coefficient. The glitches around 1 and 4.5 GHz are outside of the operation bandwidth. The average errors in the operation band of 2~4 GHz are shown in Table 4.3 (b). Most of the reconstructed results are shown in close agreement with the directly measured results except for the isolation response of  $S_{12}$ . It is because  $|S_{12}|$  is intrinsically small and a slight variation in the reconstructed result may result in a large error. Similarly, the difference of the reconstructed results from the directly measured results in  $|S_{21}|$  of Fig. 4.6(c) is mainly caused by the cable-flex repeatability in one-port measurements.

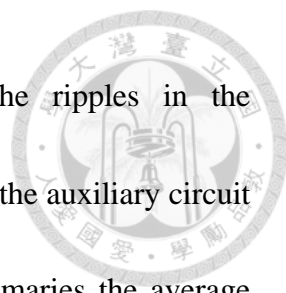
### 4.3 Two-port active DUT

In this section, an amplifier as shown in Fig. 4.7 with the use of an AVAGO ATF-54143 transistor is used as the two-port active DUT. It gives about 10dB gain in 2~4GHz range. Five one-port measurements using five auxiliary circuits are performed



as described in Section 3.2. A cable and an M-M adapter that are both characterized are used to connect the auxiliary circuit and the DUT. The cable connects the port  $P_3$  of the auxiliary circuit and the port 2 of the DUT, and the adapter connects the port  $P_2$  of auxiliary circuit and the port 1 of the DUT. Table 4.4 shows the details of five auxiliary circuits. They are composed of a three-port component and one or two two-port components. Take row (2) of Table 4.4 for example, this auxiliary circuit is a DITOM D3C2040 circulator with a 3-dB attenuation and a 6-dB attenuation connected between its port 2 and port 3. The port enumeration of DITOM D3C2040 is shown in Fig 4.8. Note one should be careful of the signal flow direction of the DITOM D3C2040 circulator in order to prevent the amplifier from oscillation. The five one-port measurements are conducted at the port 1 of an Agilent N5222A four-port VNA. It will also be used to directly measure the amplifier two-port  $S$ -matrix. The photograph of a one-port measurement setup is shown in Fig. 4.9 using the three-port auxiliary circuit given in row(1) in Table 4.4.

The reconstructed results of magnitude and phase of amplifier are shown in Fig 4.10. All the reconstructed  $S$ -parameters except for  $S_{12}$  show in close agreement with the directly measured results. The discrepancy of  $S_{12}$  is due to the signal flow direction of the DITOM D3C2040 circulator. Considering the assembly of Fig. 1.3 with a circulator as the auxiliary circuit, the circulator isolation can further suppress the weak



information of amplifier  $S_{12}$  to the VNA measured port. The ripples in the reconstructed  $S$ -parameters are also due to the cable used to connect the auxiliary circuit and the two-port DUT as discussed in Section 4.1. Table 4.5 summaries the average errors of amplifier in the operation band of 1~5GHz. The large error of  $S_{12}$  is because  $|S_{12}|$  is intrinsically small and the effect of circulator used in the measurements.

#### 4.4 Three-port reciprocal network using comparison process

The fourth example of a three-port reciprocal DUT is given in this section to verify the reconstruction method described in Section 2.3. In this case, an Agilent 11667B power splitter is used as the three-port reciprocal DUT. A total of nine one-port measurements are performed at the port 1 of a four-port Agilent N5230A VNA. The open and short standards in Agilent 85052D calibration kit are used as the known terminations for the seven one-port measurements as described in Table 2.1. A characterized coaxial cable is used as the two-port auxiliary circuit. The three-port direct measurement of DUT is also performed for the comparison of those results using the developed one-port comparison method described in Section 2.3. (4.1) is used to calculate the average error of each  $S$ -parameter.

The reconstructed results of magnitude and phase from 2 to 10 GHz are shown in Fig.11. Table 4.5 lists the average errors of the resulted nine  $S$ -parameters of the DUT. Note that because  $|S_{11}|$  is quite small, according to (4.1), a slight variation during the



one-port measurements could result in large error in percentage.

## 4.5 Summary

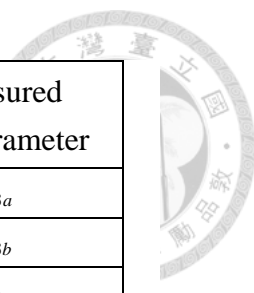
This chapter presents the experimental results of two three-port passive DUTs and an active two-port amplifier. The deviations of the reconstructed results are explained. It shows that by applying the type-II PRM, one can reconstruct the multiport  $S$ -matrix of the DUT from one-port measurements.

Note other reconstruction methods such as the one in [5] and the type-III PRM [9] can also be applied to solve the  $n$ -port  $S$ -matrix from the two-port intermediate  $S$ -matrices. Take the type-III PRM for example. Since each port of the DUT is terminated once in the type-III PRM while the type-II PRM terminates twice at one port and once at another port, the type-III PRM can reduce the error difference between the solved diagonal elements. As for the consideration of the number of one-port measurements, the method in [5] needs  $C_2^n \times 4$  to  $C_2^n \times 5$  one-port measurements while the type-II PRM needs about  $4 \times 3^{n-2}$  to  $5 \times 3^{n-2}$  one-port measurements. Therefore, for a DUT with large number of ports, one may consider to use the method in [5].

In addition, it makes sense that the magnitude of the measured data should be large enough to be properly analyzed. In the presented experimental examples, the smallest measured data are about -35dB. The threshold level of the measured data to solve the

correct results needs further study.



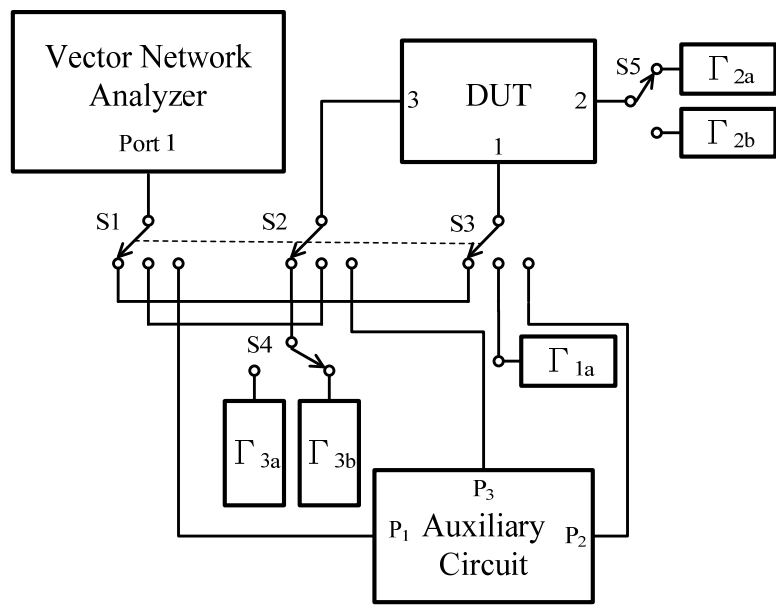


Port of resulting three-port S-matrix	Port of intermediate two-port S-matrix	Port of measured one-port S-parameter
123	$13\_ \Gamma_{2a}$	$1\_ \Gamma_{2a} \Gamma_{3a}$
		$1\_ \Gamma_{2a} \Gamma_{3b}$
		$3\_ \Gamma_{1a} \Gamma_{2a}$
		$P_1\_ P_2 \Gamma_{2a} P_3$
	$13\_ \Gamma_{2b}$	$1\_ \Gamma_{2b} \Gamma_{3a}$
		$1\_ \Gamma_{2b} \Gamma_{3b}$
		$3\_ \Gamma_{1a} \Gamma_{2b}$
		$P_1\_ P_2 \Gamma_{2b} P_3$
	$12\_ \Gamma_{3a}$	$1\_ \Gamma_{2a} \Gamma_{3a}^*$
		$1\_ \Gamma_{2b} \Gamma_{3a}^*$
		$2\_ \Gamma_{1a} \Gamma_{3a}$
		$P_1\_ P_2 P_3 \Gamma_{3a}$

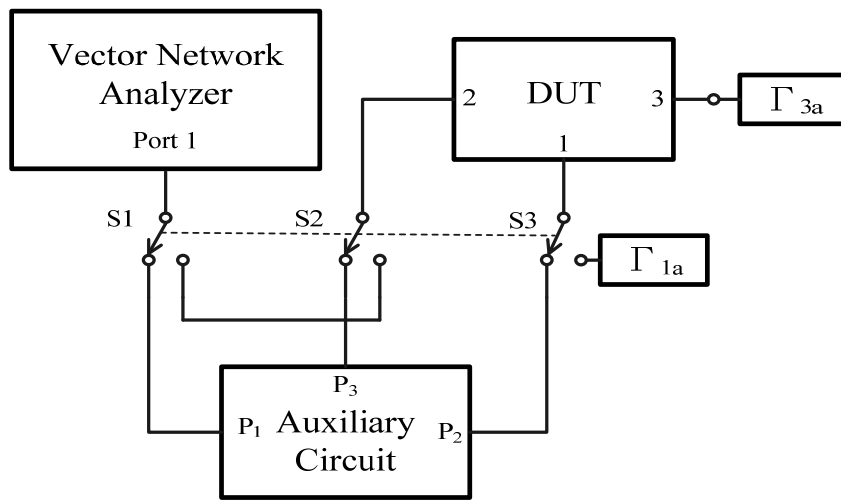
Table 4.1 Port description of the scattering matrices.

	Reciprocal DUT	Non-reciprocal DUT
DUT	Power splitter (Agilent 11667B)	Circulator (DITOM D3I2040)
Auxiliary circuit	Power splitter (Agilent 11667B) with a short cable and an M-M adapter	
$\Gamma_{1a}$	Short termination with a 3-dB attenuator	
$\Gamma_{2a}$	Open termination with a 5-dB attenuator	
$\Gamma_{2b}$	Short termination with a 6-dB attenuator	
$\Gamma_{3a}$	Open termination with a 3-dB attenuator	
$\Gamma_{3b}$	Short termination with an M-M adaptor	

Table 4.2 Details of components for three-port DUT examples.



(a)



(b)

Fig. 4.1. Measurement arrangements for (a) the first eight and (b) the last two one-port  $S$ -matrix measurements given in the right column of Table 4.1.

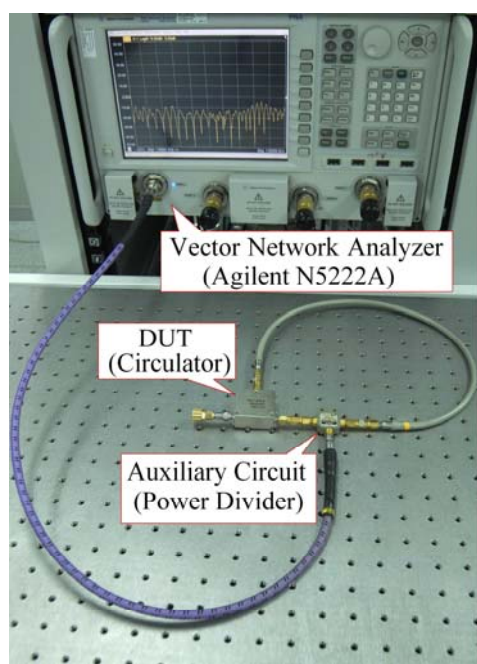


Fig. 4.2 Photograph of a one-port measurement setup.

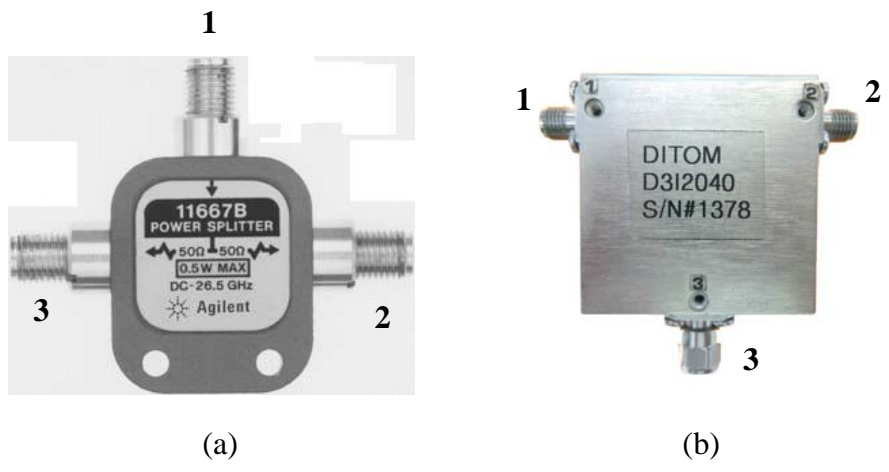
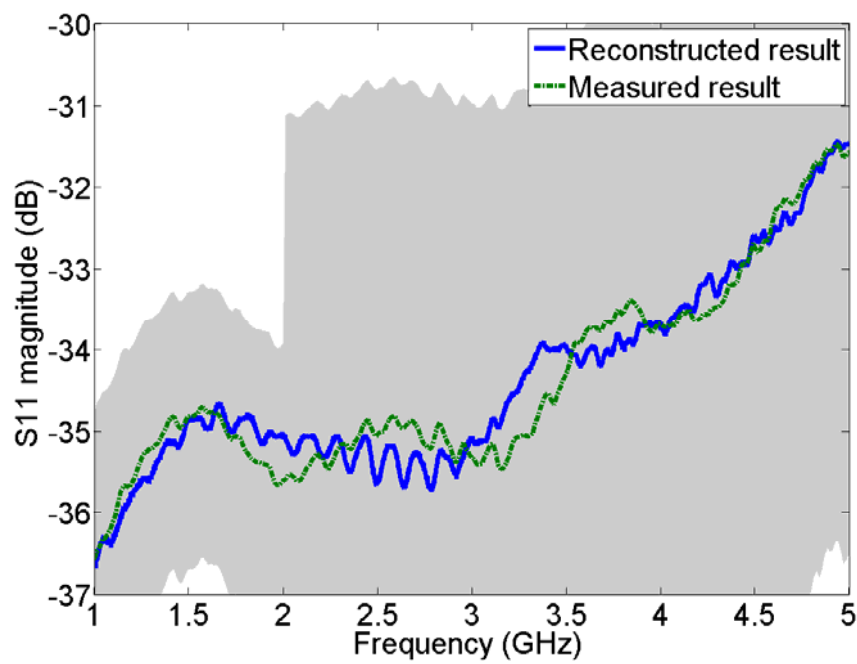
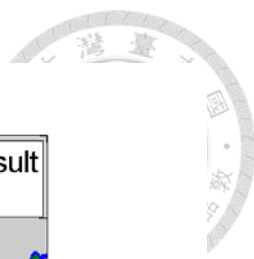
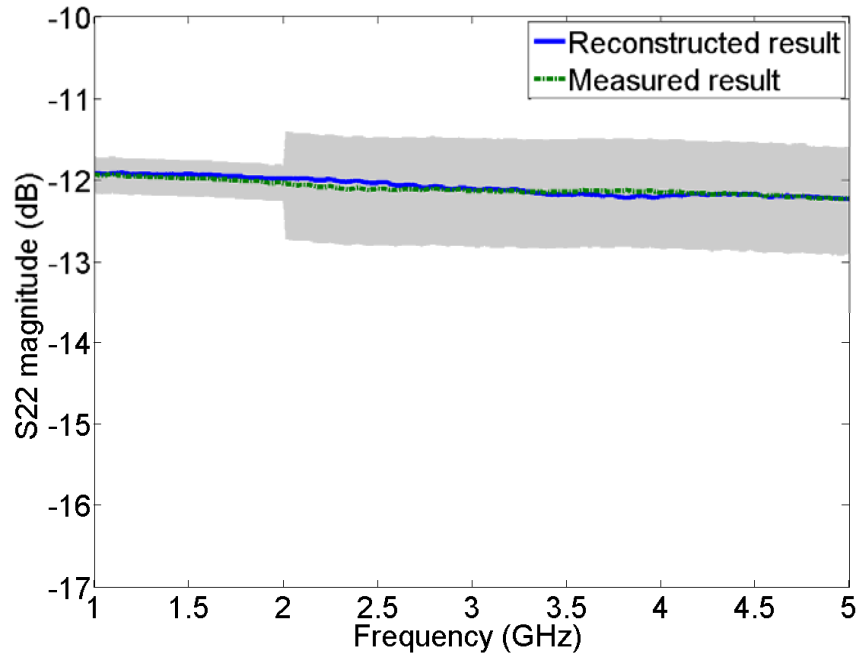


Fig. 4.3 Port enumeration of (a) Agilent 11667B power splitter and (b) DITOM D3I2040 circulator.



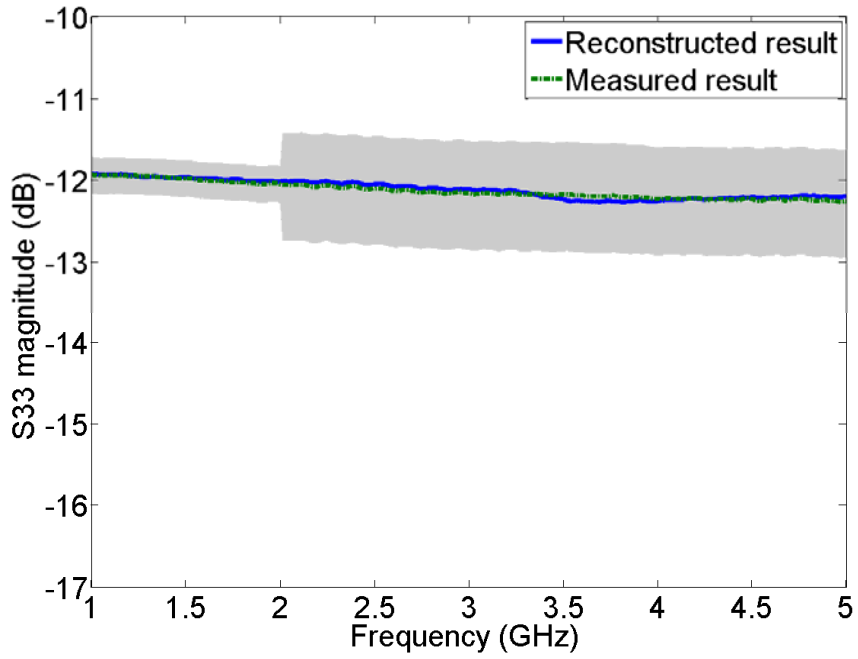


(a)

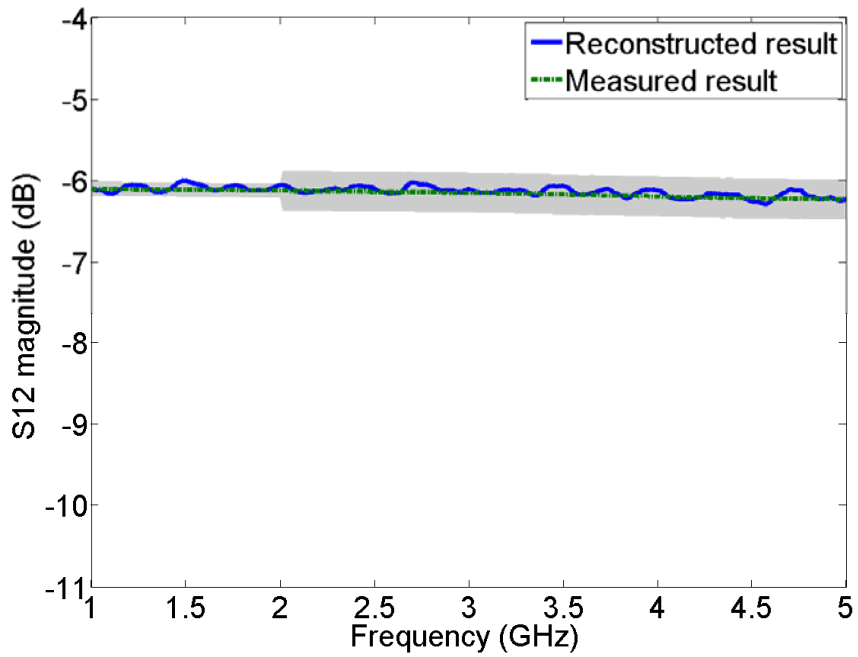


(b)

Fig. 4.4 Reconstructed results of magnitude of (a)  $S_{11}$ , (b)  $S_{22}$ , (c)  $S_{33}$ , (d)  $S_{12}$ , (e)  $S_{13}$ , and (f)  $S_{23}$  of an Agilent 11667B power splitter.

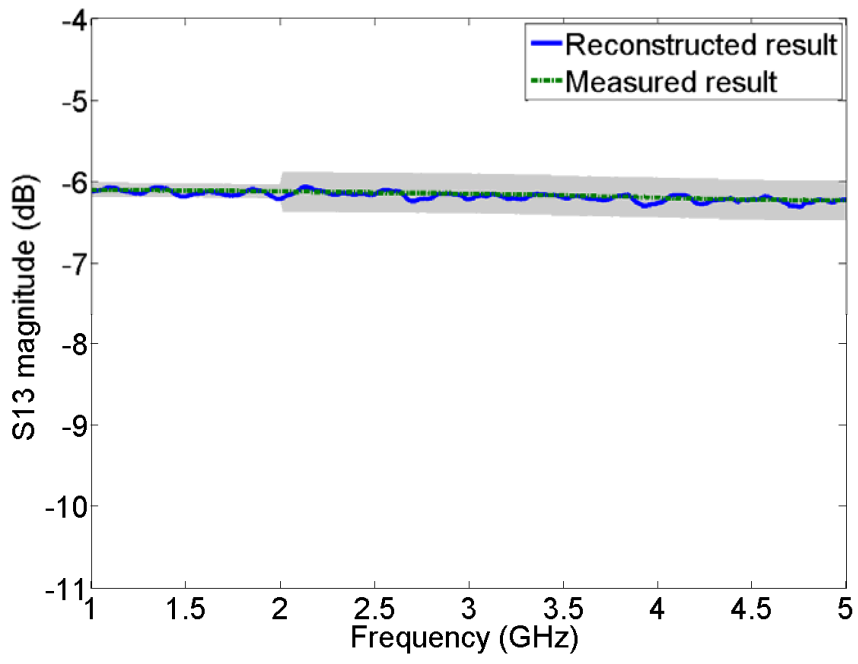


(c)

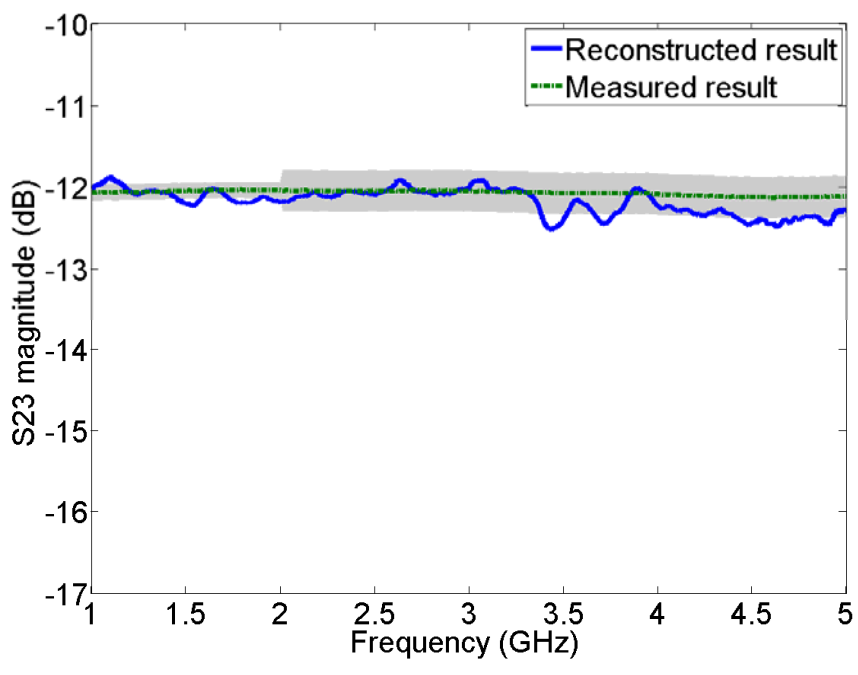


(d)

Fig. 4.4 Reconstructed results of magnitude of (a)  $S_{11}$ , (b)  $S_{22}$ , (c)  $S_{33}$ , (d)  $S_{12}$ , (e)  $S_{13}$ , and (f)  $S_{23}$  of an Agilent 11667B power splitter.

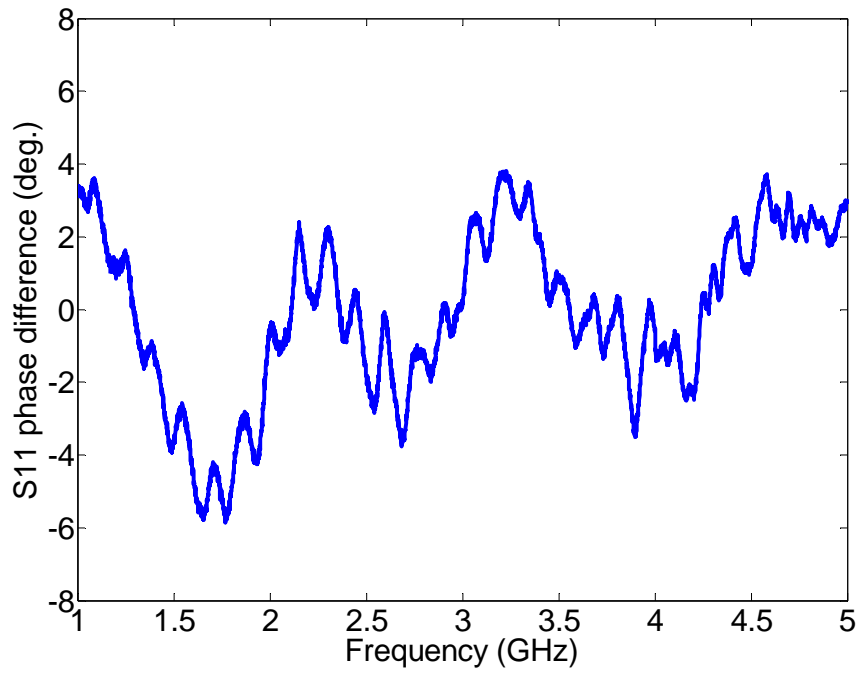
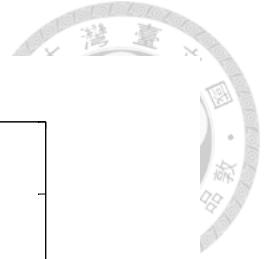


(e)

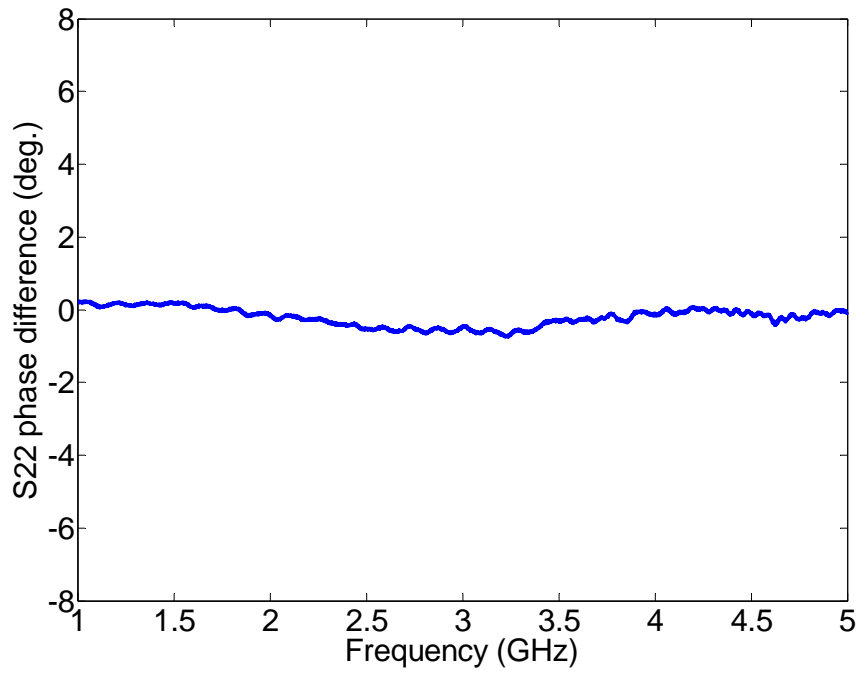


(f)

Fig. 4.4 Reconstructed results of magnitude of (a)  $S_{11}$ , (b)  $S_{22}$ , (c)  $S_{33}$ , (d)  $S_{12}$ , (e)  $S_{13}$ , and (f)  $S_{23}$  of an Agilent 11667B power splitter.

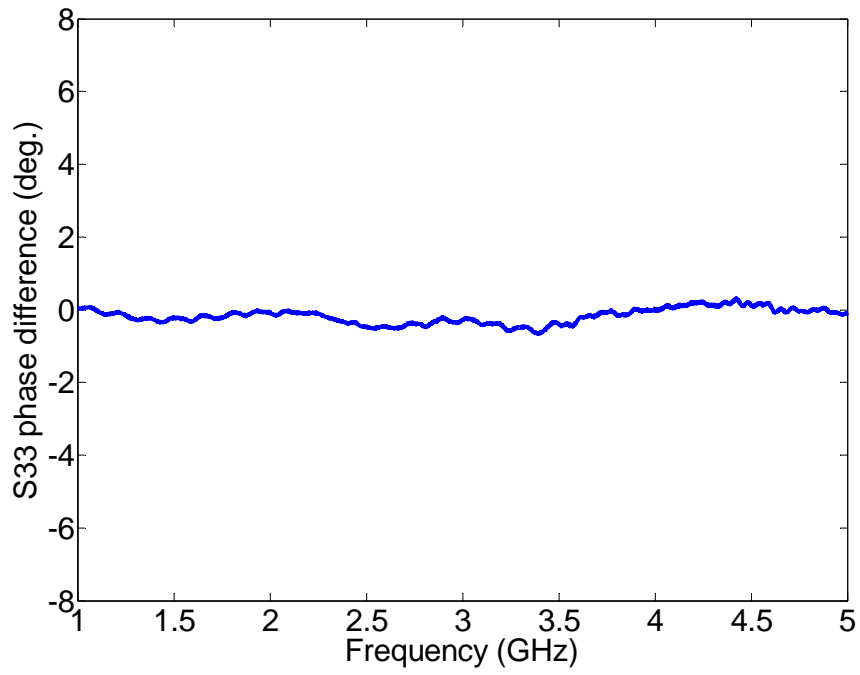
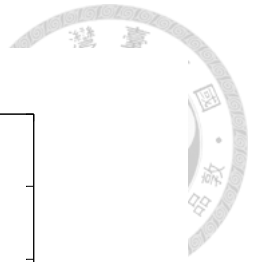


(a)

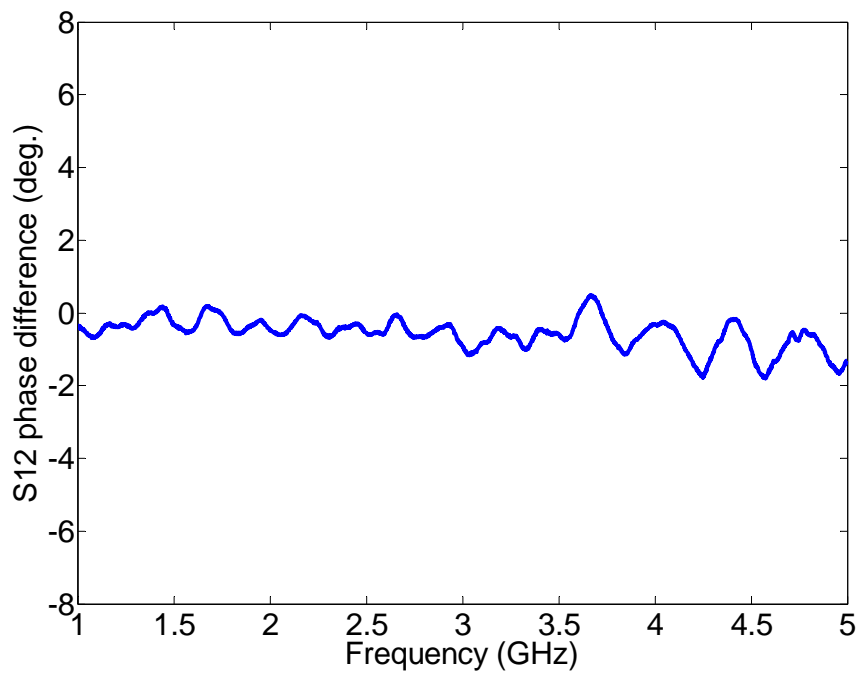


(b)

Fig. 4.5 Phase difference of reconstructed and measured results of (a)  $S_{11}$ , (b)  $S_{22}$ , (c)  $S_{33}$ , (d)  $S_{12}$ , (e)  $S_{13}$ , and (f)  $S_{23}$  of an Agilent 11667B power splitter.

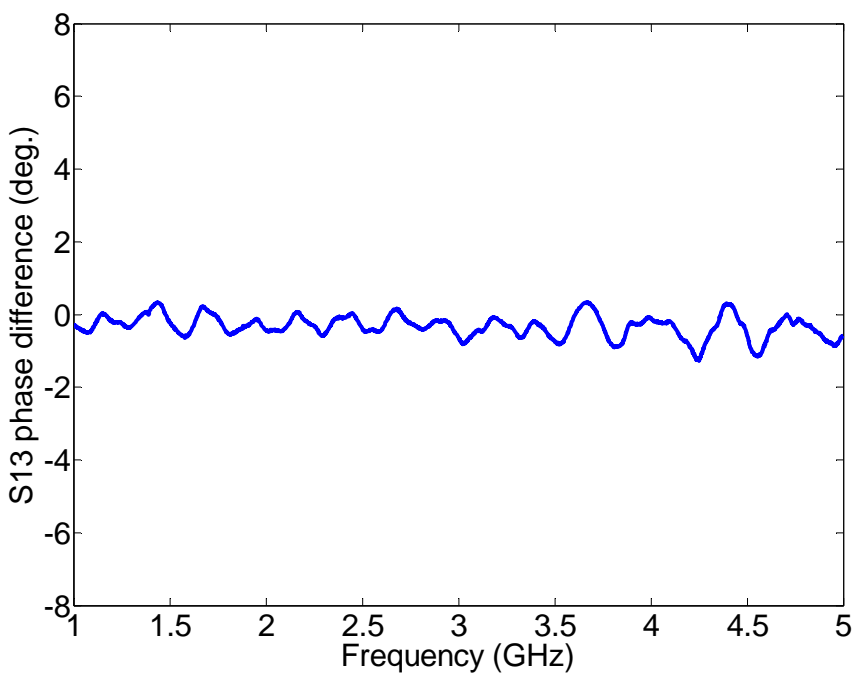
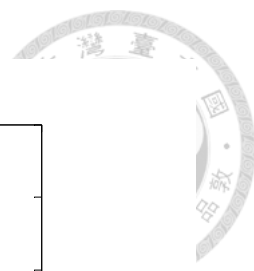


(c)

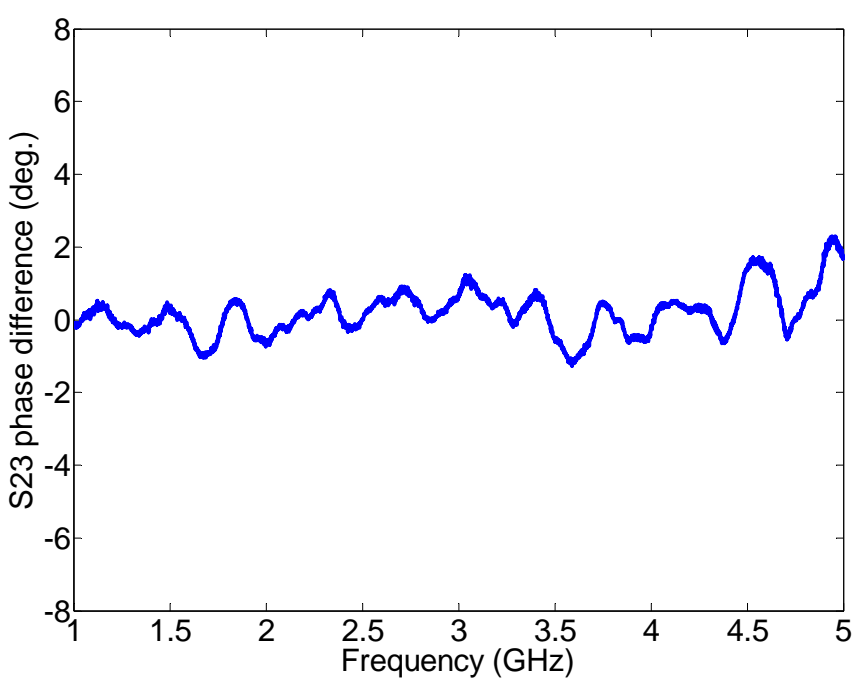


(d)

Fig. 4.5 Phase difference of reconstructed and measured results of (a)  $S_{11}$ , (b)  $S_{22}$ , (c)  $S_{33}$ , (d)  $S_{12}$ , (e)  $S_{13}$ , and (f)  $S_{23}$  of an Agilent 11667B power splitter.



(e)



(f)

Fig. 4.5 Phase difference of reconstructed and measured results of (a)  $S_{11}$ , (b)  $S_{22}$ , (c)  $S_{33}$ , (d)  $S_{12}$ , (e)  $S_{13}$ , and (f)  $S_{23}$  of an Agilent 11667B power splitter.



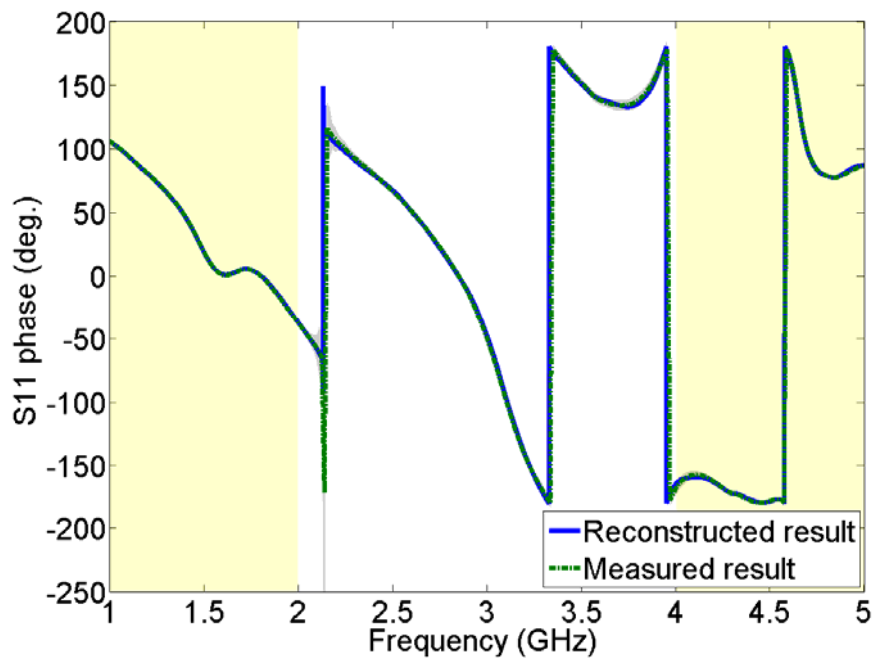
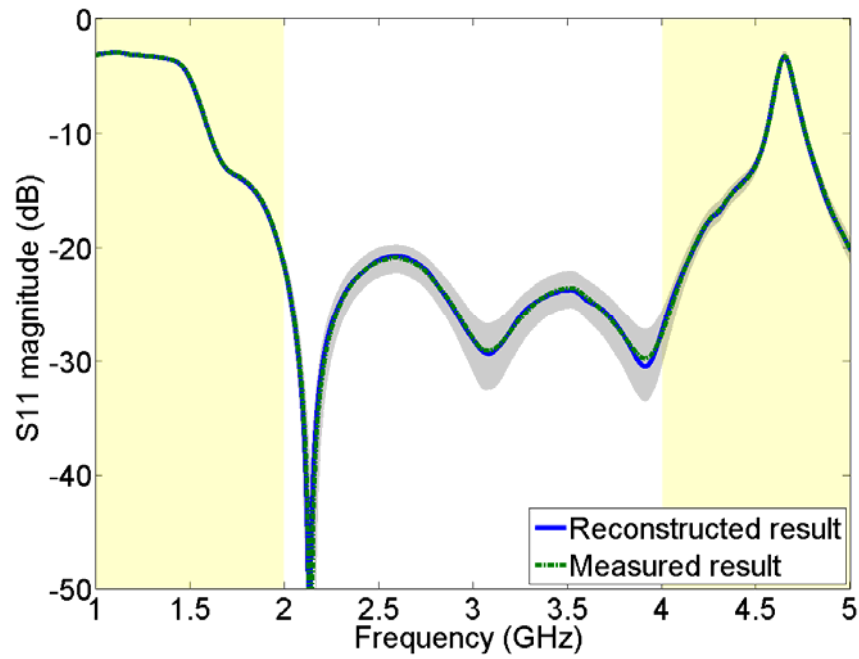
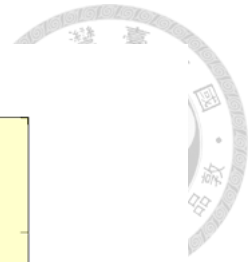
Average errors (%) of reciprocal DUT		
$S_{11}$ :5.05	$S_{12}$ :1.15	$S_{13}$ :0.80
$S_{21}$ :1.09	$S_{22}$ :0.70	$S_{23}$ :1.19
$S_{31}$ :0.82	$S_{32}$ :1.17	$S_{33}$ :0.60

(a)

Average errors (%) of nonreciprocal DUT		
$S_{11}$ :5.97	$S_{12}$ :9.15	$S_{13}$ :0.82
$S_{21}$ :1.34	$S_{22}$ :2.85	$S_{23}$ :8.94
$S_{31}$ :3.03	$S_{32}$ :1.15	$S_{33}$ :1.85

(b)

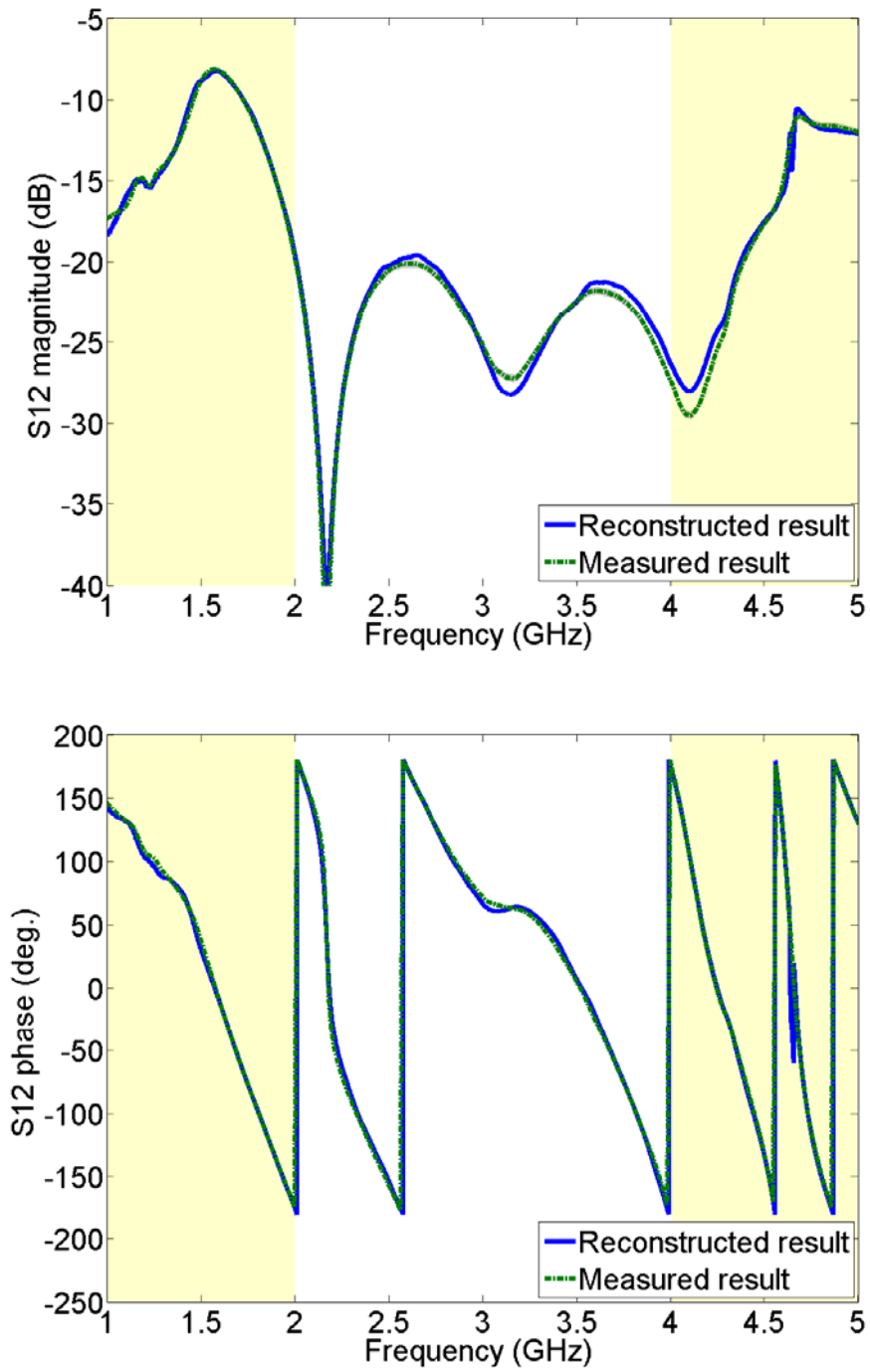
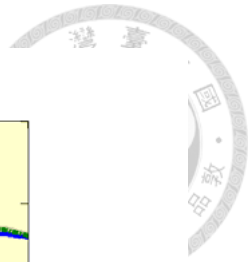
Table 4.3 Average errors of the first two examples of three-port (a) reciprocal and (b) nonreciprocal DUTs.



(a)

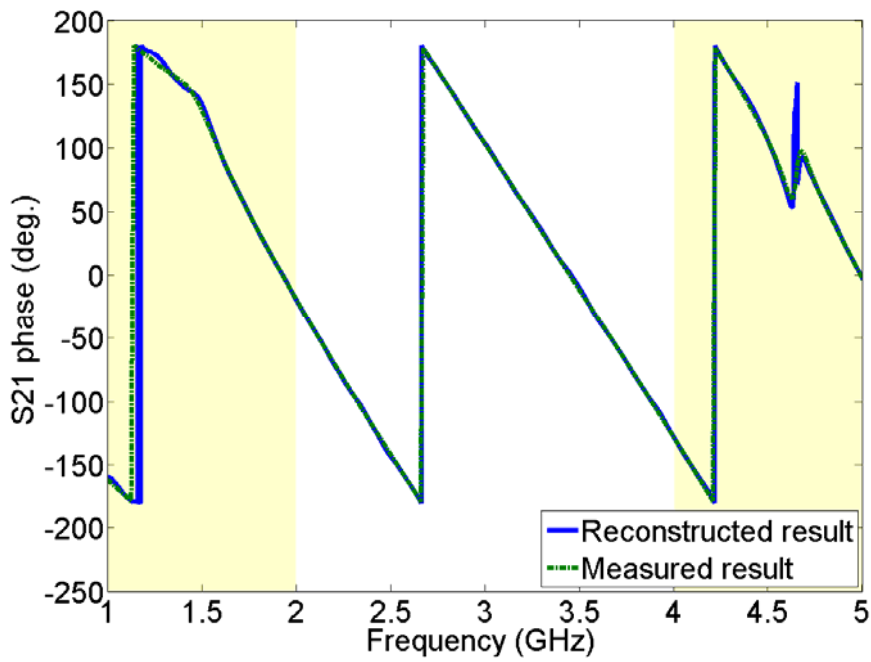
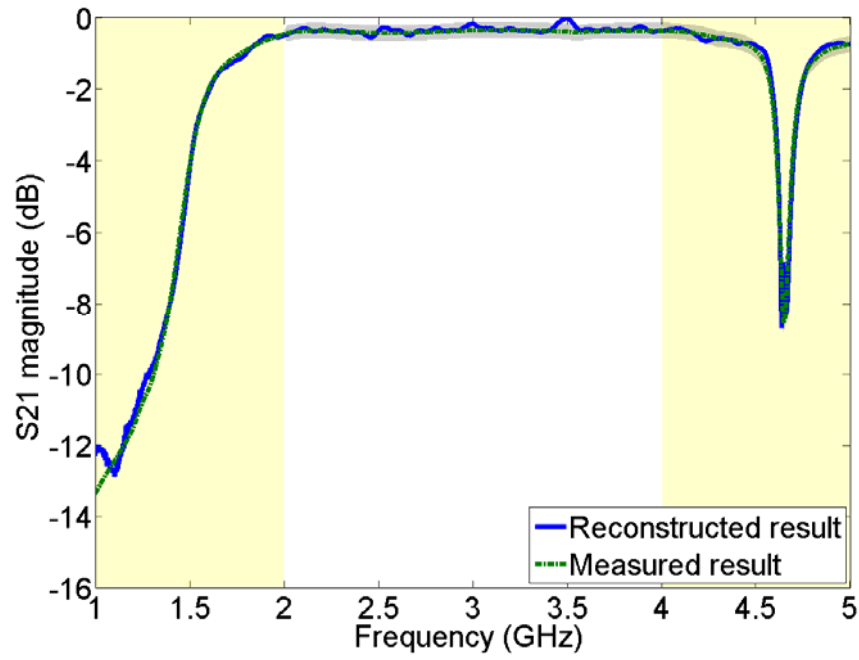
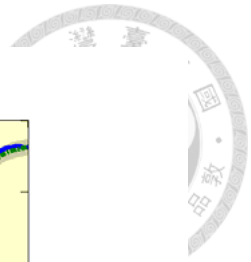
Fig. 4.6 Reconstructed results of (a)  $S_{11}$ , (b)  $S_{12}$ , and (c)  $S_{21}$  of a DITOM D3I2040 circulator.





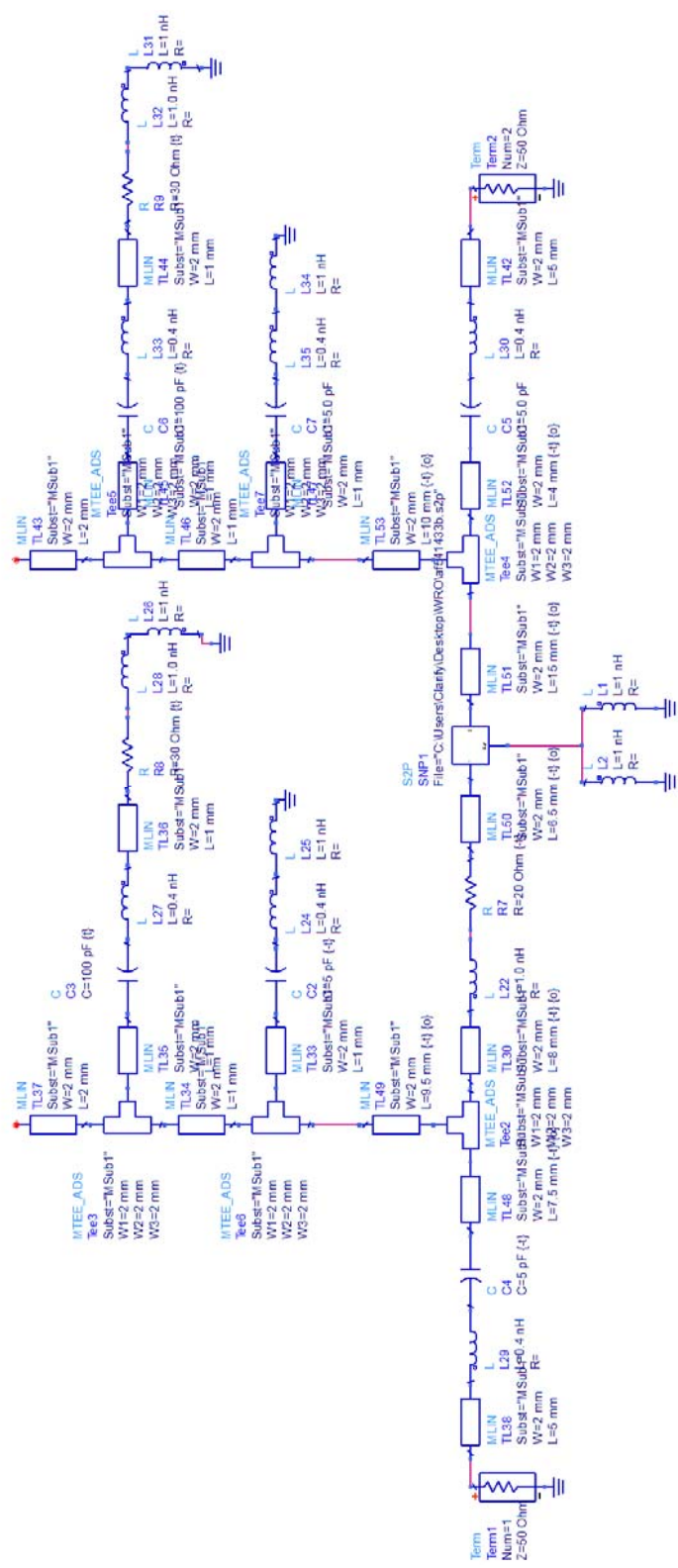
(b)

Fig. 4.6 Reconstructed results of (a)  $S_{11}$ , (b)  $S_{12}$ , and (c)  $S_{21}$  of a DITOM D3I2040 circulator.



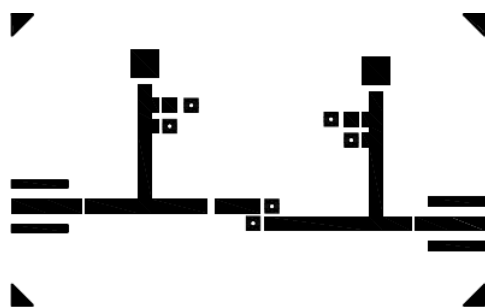
(c)

Fig. 4.6 Reconstructed results of (a)  $S_{11}$ , (b)  $S_{12}$ , and (c)  $S_{21}$  of a DITOM D3I2040 circulator.

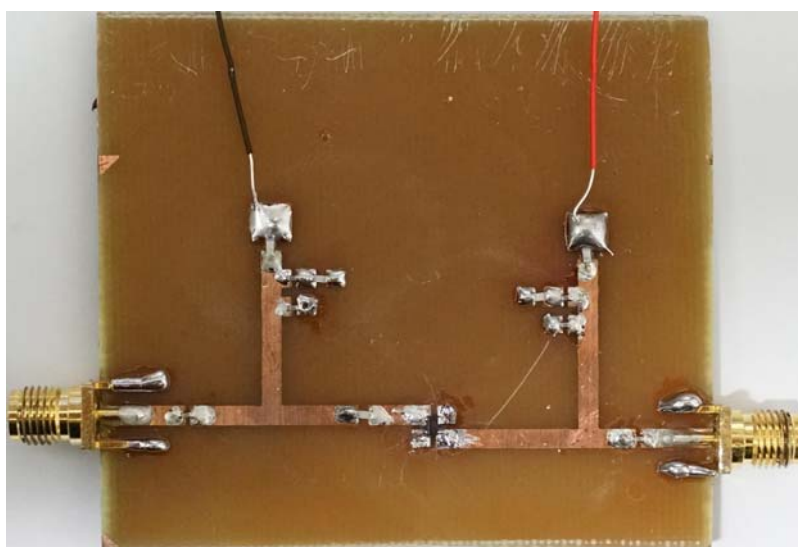


(a)

Fig. 4.7 (a) Schematic diagram, (b) layout and (c) photograph of amplifier.



(b)



(a)

Fig. 4.7 (a) Schematic diagram, (b) layout and (c) photograph of amplifier.



(b)

Fig. 4.8 Port enumeration of DITOM D3C2040 circulator.

Auxiliary circuits			
Three-port component component	Port 1	Port 2	Port 3
(1) DITOM D3C2040		6-dB attenuator	
(2) DITOM D3C2040		3-dB attenuator	6-dB attenuator
(3) Agilent 11667B	3-dB attenuator		
(4) Agilent 11667B	3-dB attenuator		M-F adapter
(5) Agilent 11667B	3-dB attenuator	3-dB attenuator	

Table 4.4 Details of components of five auxiliary circuits.

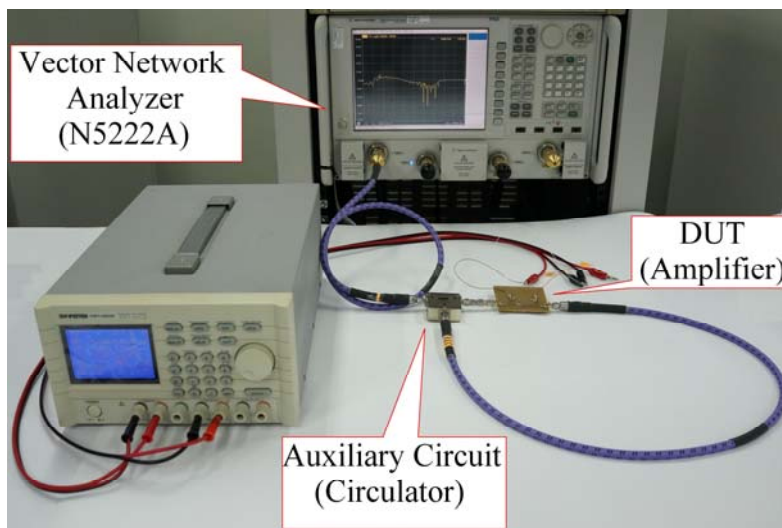
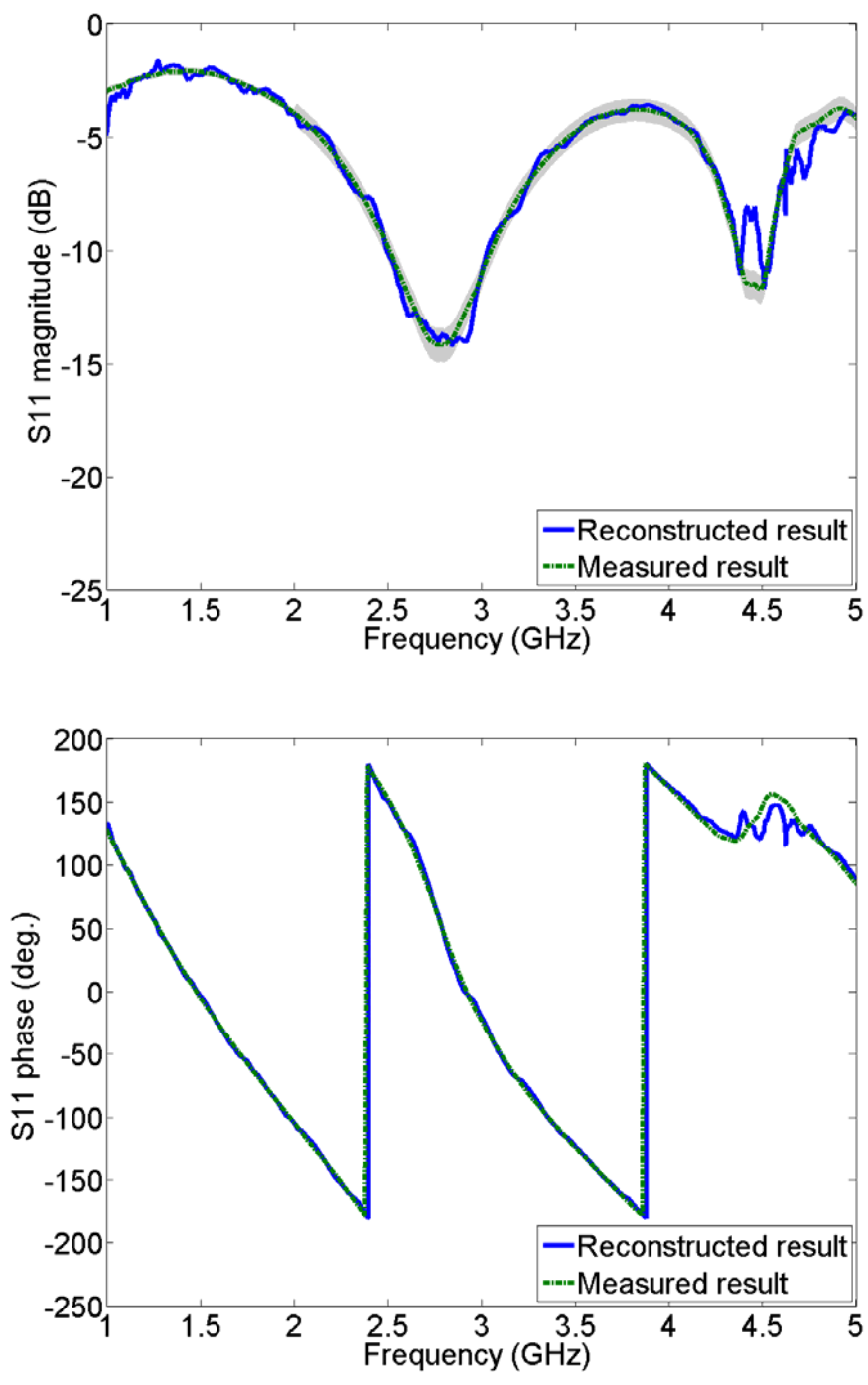
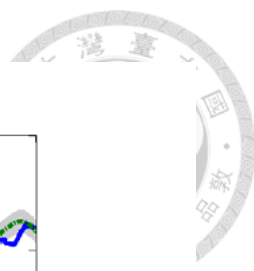
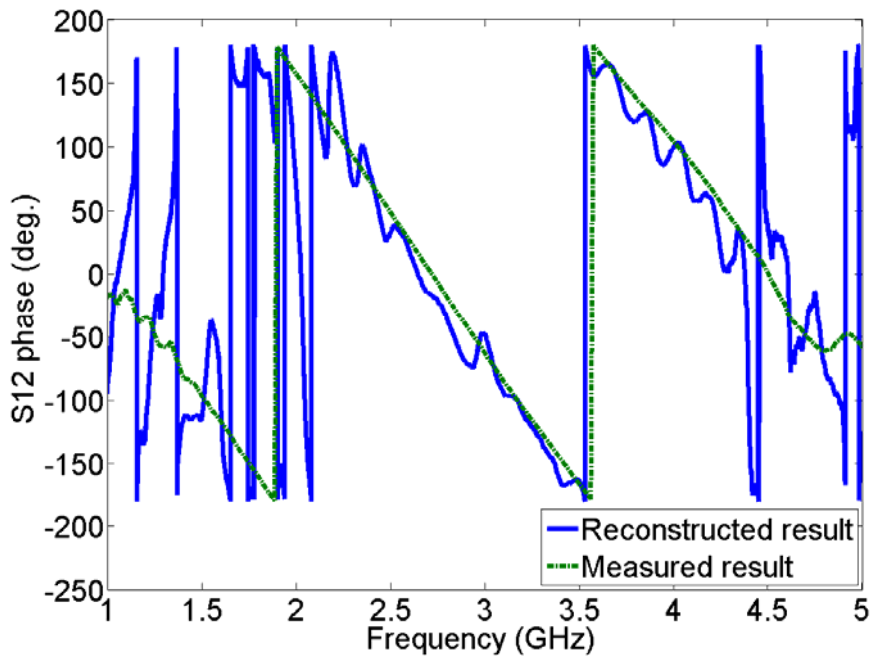
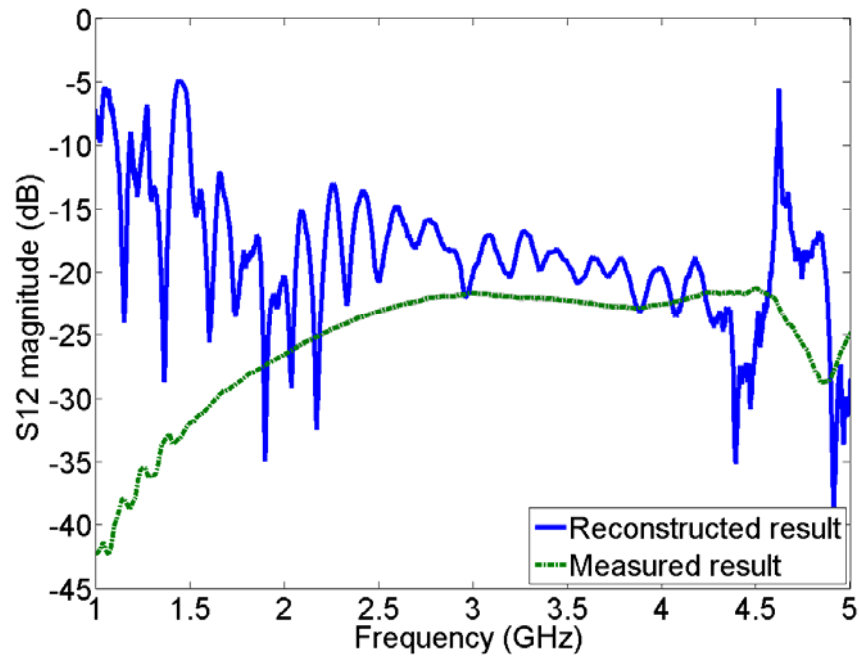
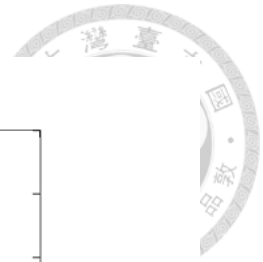


Fig. 4.9 Photograph of a one-port measurement setup for two-port active DUT example.



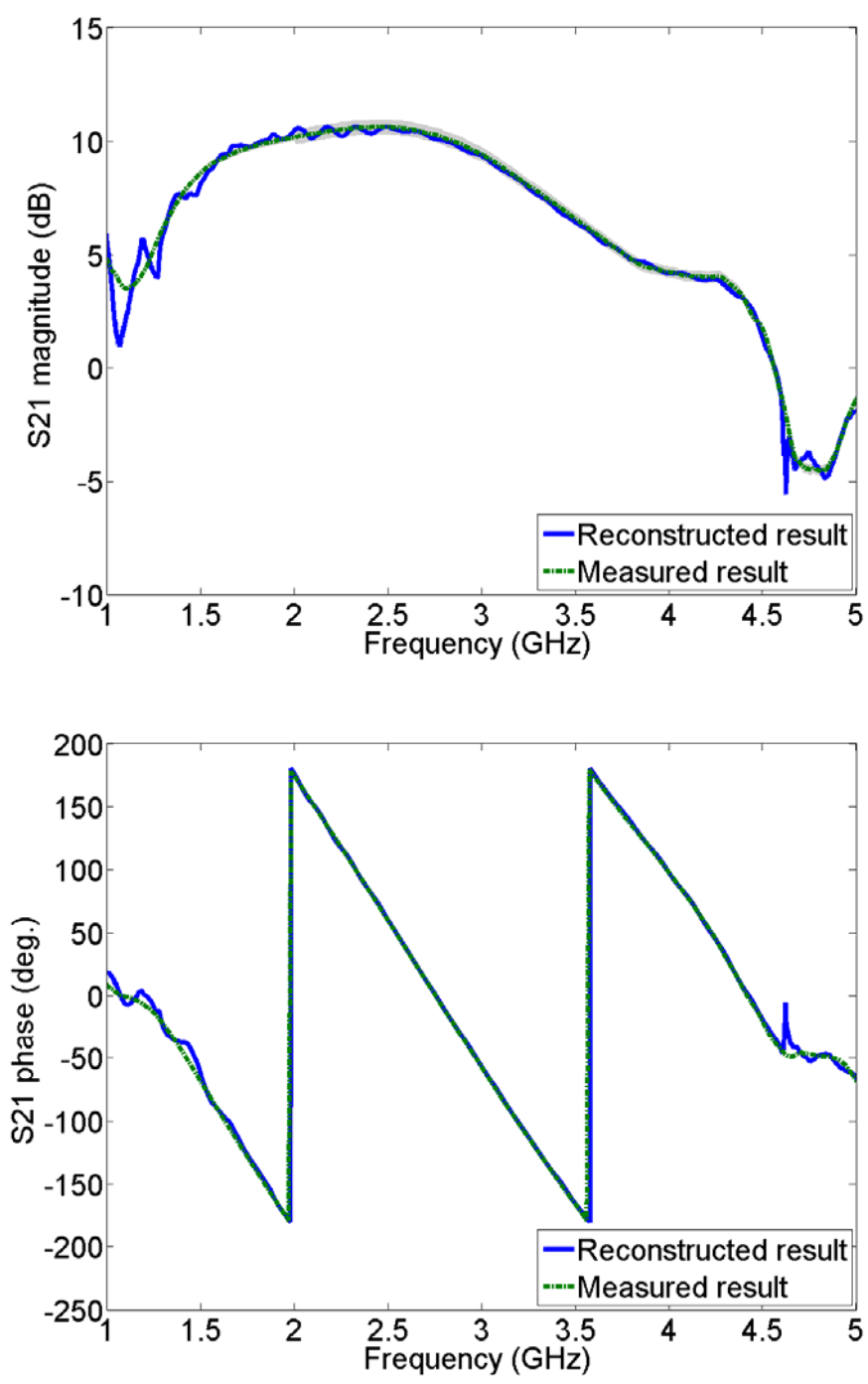
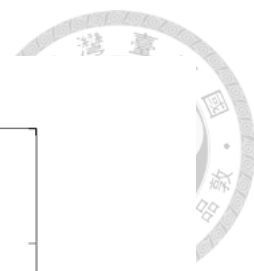
(a)

Fig. 4.10 Reconstructed results of (a)  $S_{11}$ , (b)  $S_{12}$ , (c)  $S_{21}$ , and (d)  $S_{22}$  of amplifier.



(b)

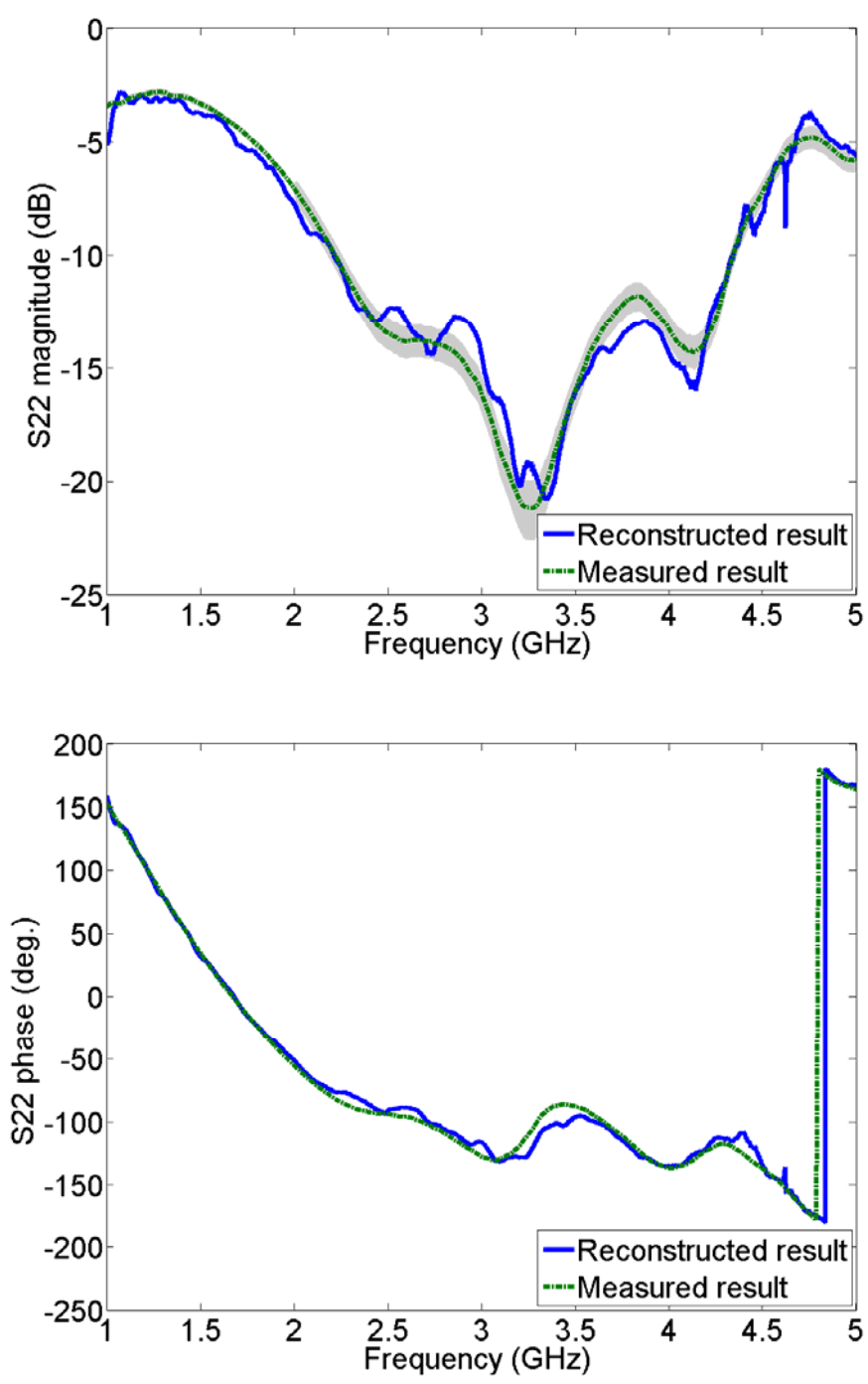
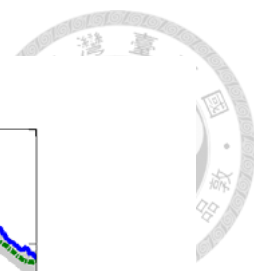
Fig. 4.10 Reconstructed results of (a)  $S_{11}$ , (b)  $S_{12}$ , (c)  $S_{21}$ , and (d)  $S_{22}$  of amplifier.



(c)

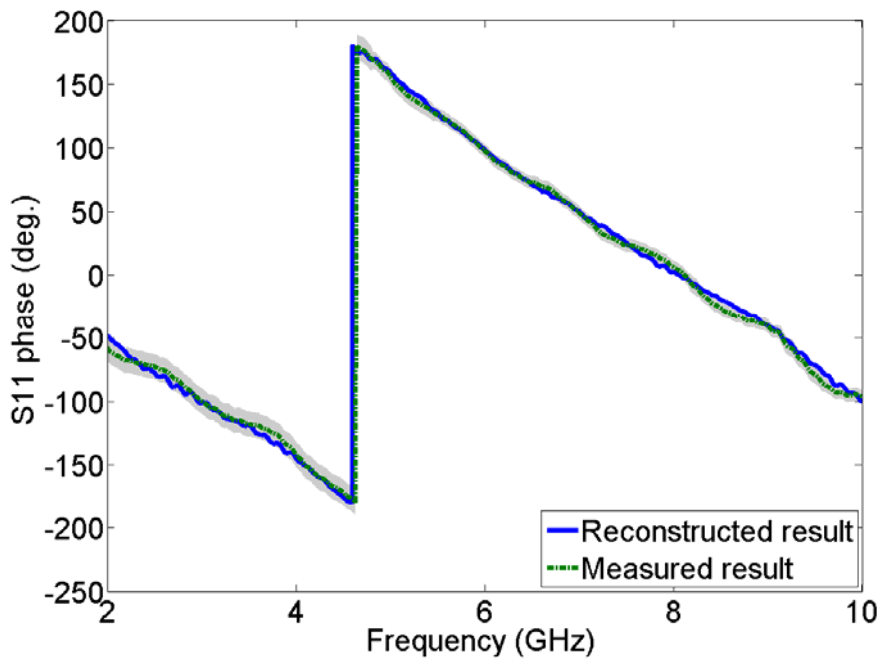
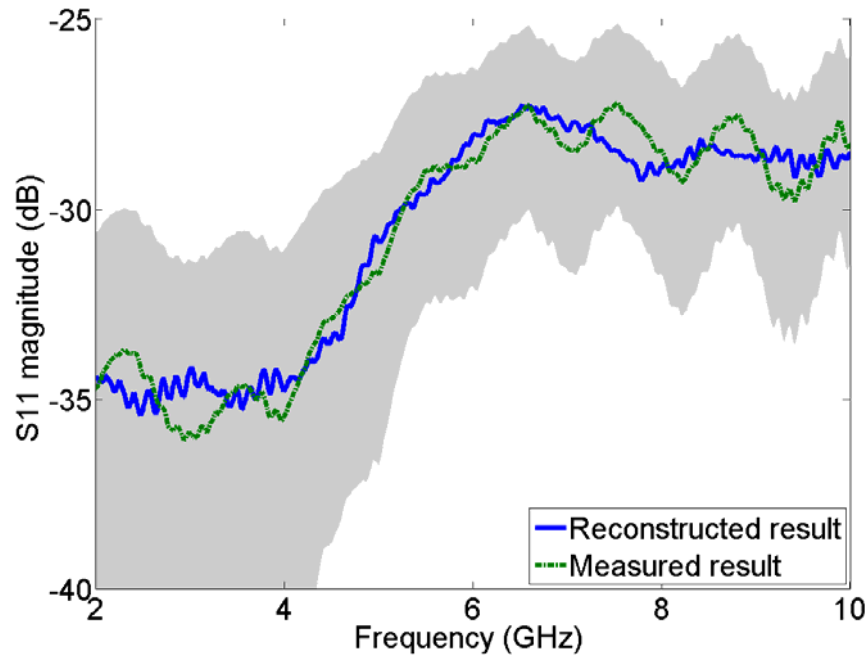
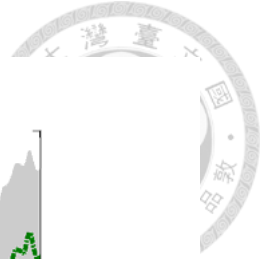
Fig. 4.10 Reconstructed results of (a)  $S_{11}$ , (b)  $S_{12}$ , (c)  $S_{21}$ , and (d)  $S_{22}$  of amplifier.





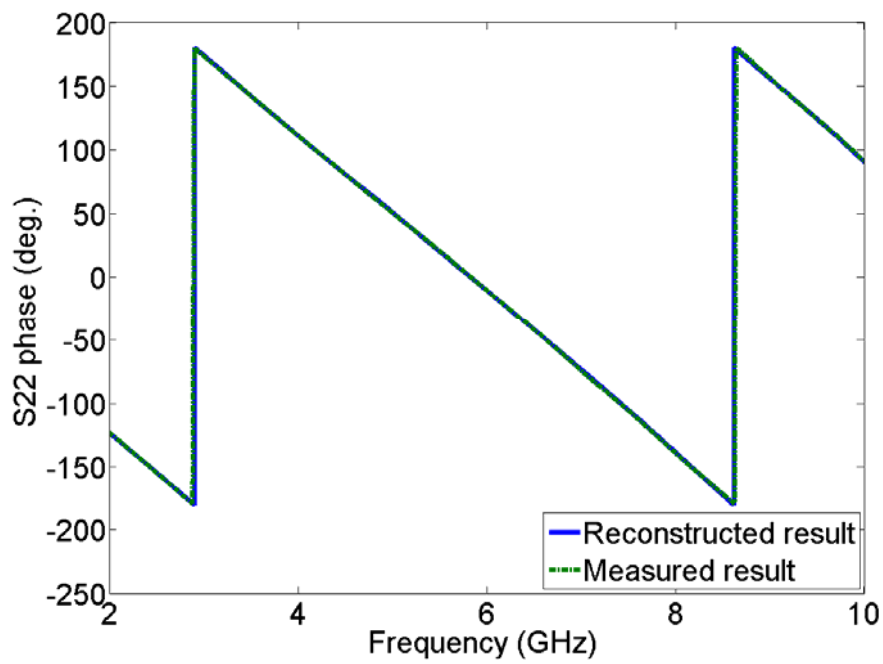
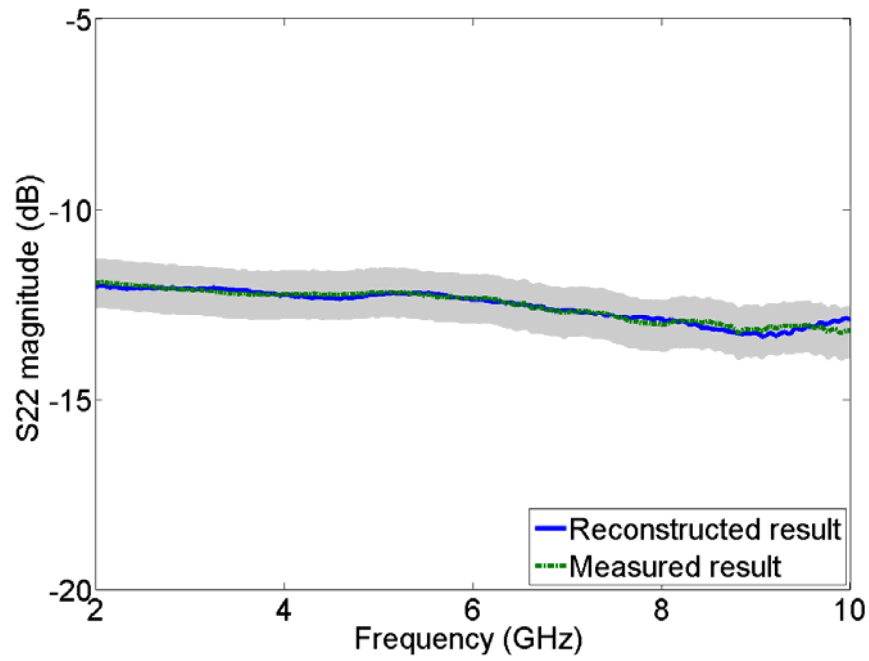
(d)

Fig. 4.10 Reconstructed results of (a)  $S_{11}$ , (b)  $S_{12}$ , (c)  $S_{21}$ , and (d)  $S_{22}$  of amplifier.



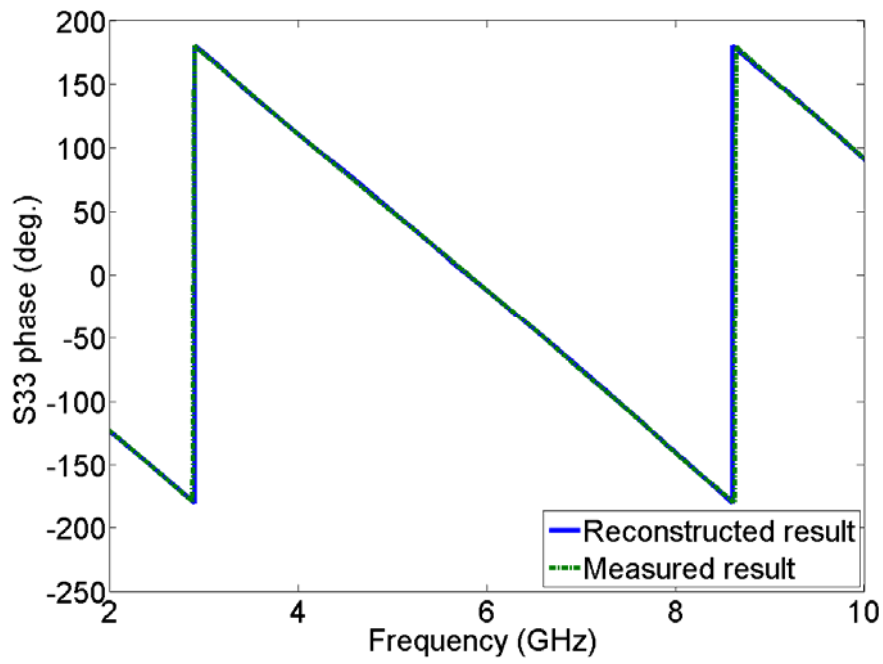
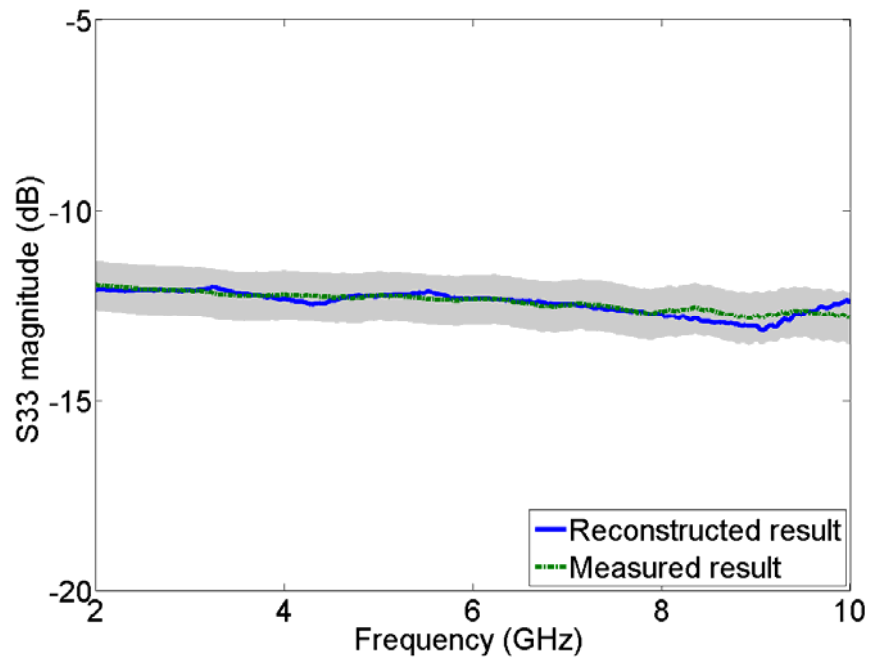
(a)

Fig. 4.11 Reconstructed results of (a)  $S_{11}$ , (b)  $S_{22}$ , (c)  $S_{33}$ , (d)  $S_{21}$ , (e)  $S_{31}$ , and (f)  $S_{32}$  of an Agilent 11667B power splitter.



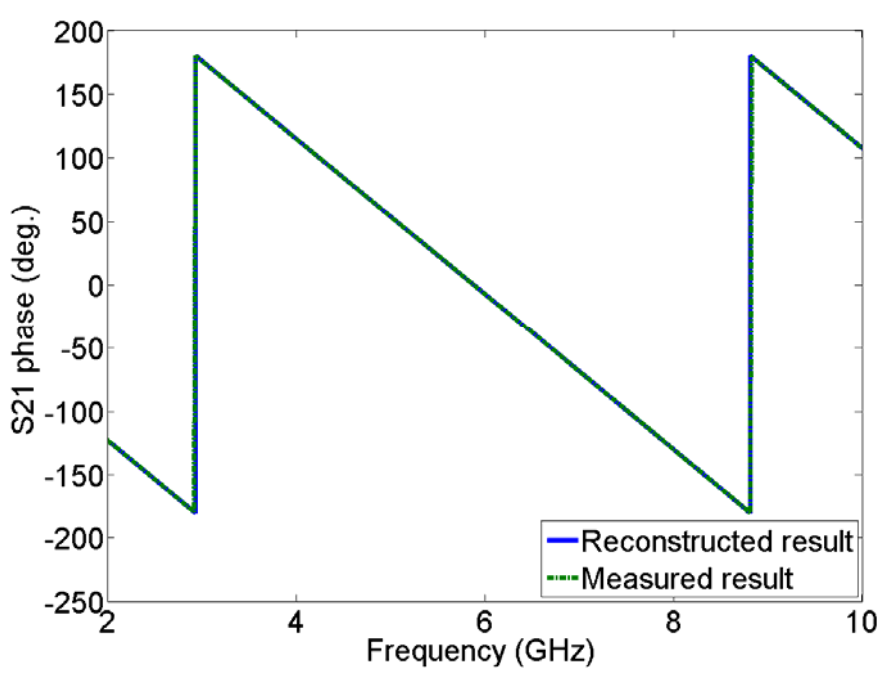
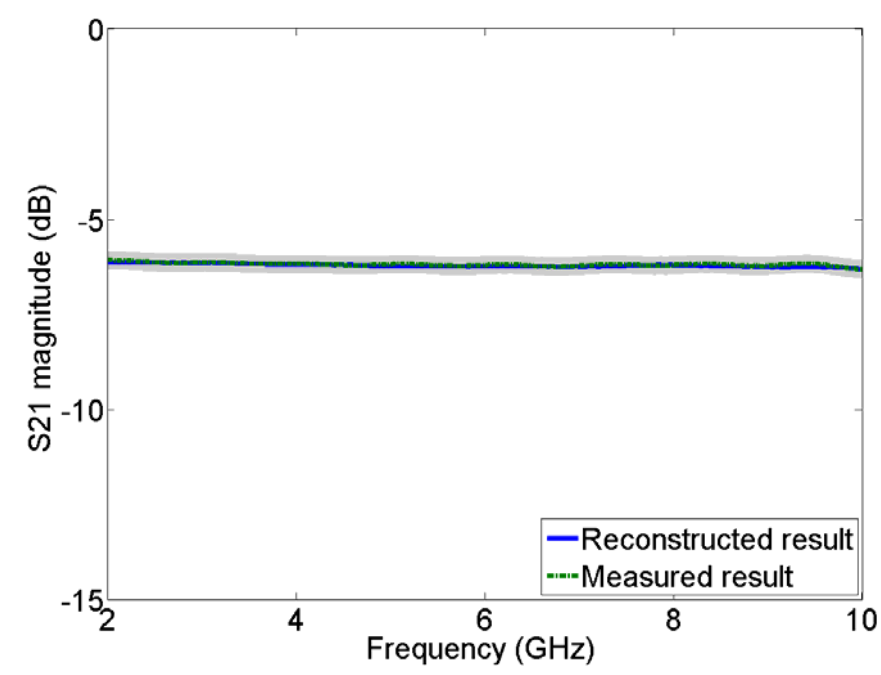
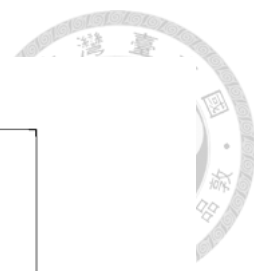
(b)

Fig. 4.11 Reconstructed results of (a)  $S_{11}$ , (b)  $S_{22}$ , (c)  $S_{33}$ , (d)  $S_{21}$ , (e)  $S_{31}$ , and (f)  $S_{32}$  of an Agilent 11667B power splitter.



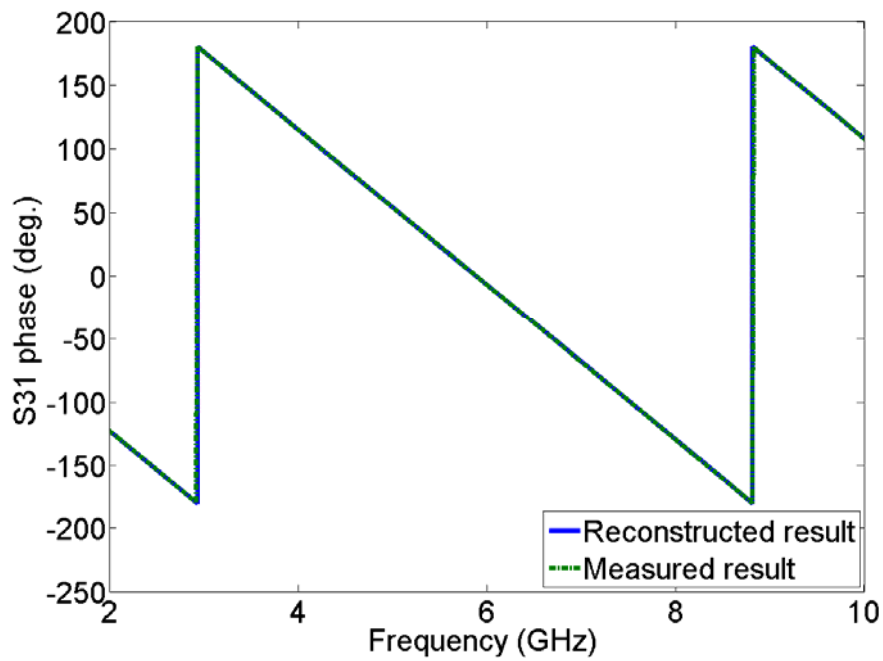
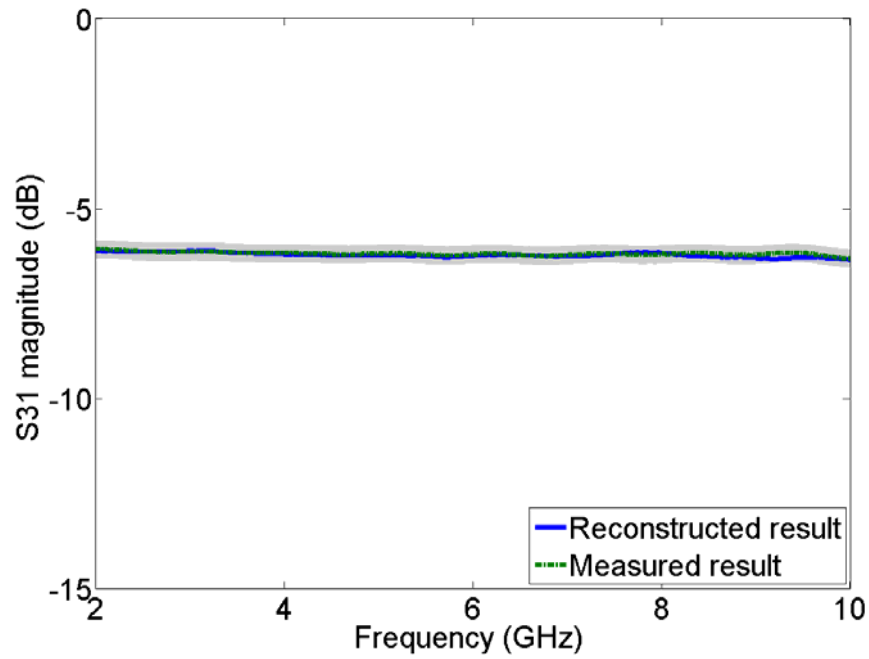
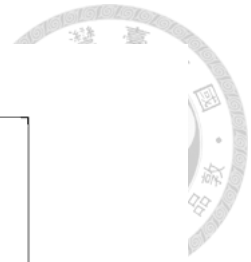
(c)

Fig. 4.11 Reconstructed results of (a)  $S_{11}$ , (b)  $S_{22}$ , (c)  $S_{33}$ , (d)  $S_{21}$ , (e)  $S_{31}$ , and (f)  $S_{32}$  of an Agilent 11667B power splitter.



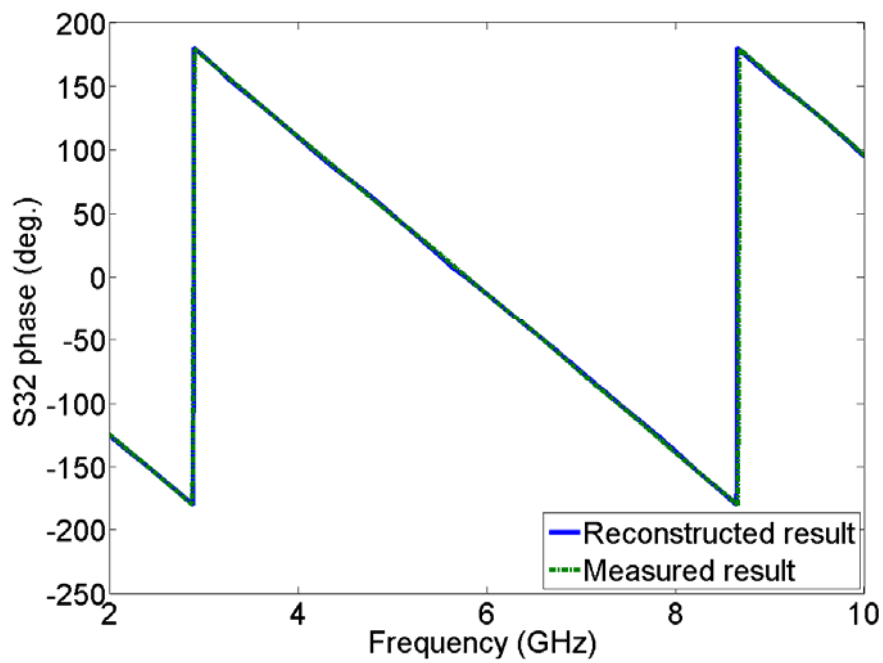
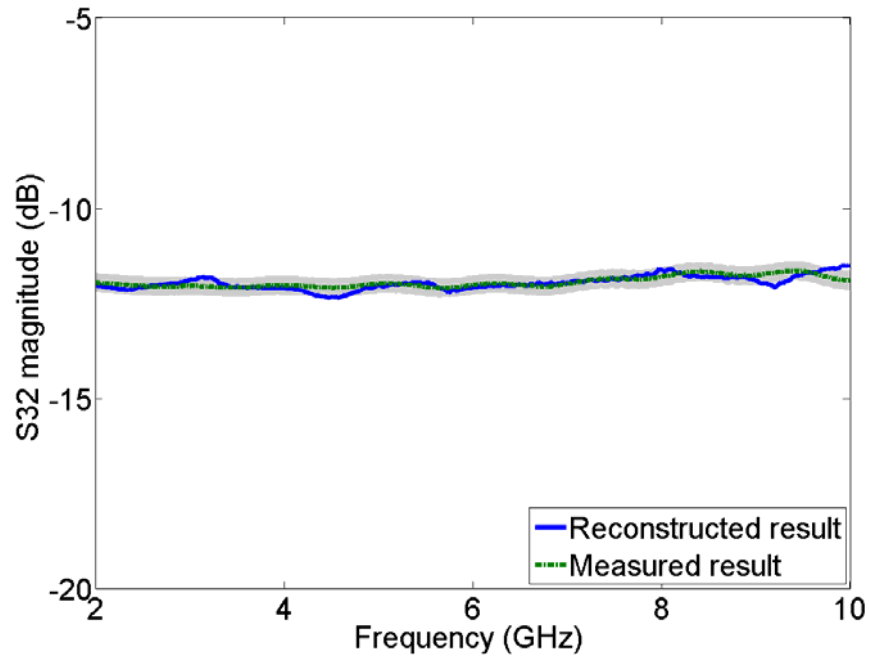
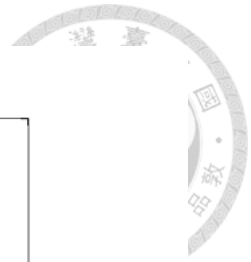
(d)

Fig. 4.11 Reconstructed results of (a)  $S_{11}$ , (b)  $S_{22}$ , (c)  $S_{33}$ , (d)  $S_{21}$ , (e)  $S_{31}$ , and (f)  $S_{32}$  of an Agilent 11667B power splitter.



(e)

Fig. 4.11 Reconstructed results of (a)  $S_{11}$ , (b)  $S_{22}$ , (c)  $S_{33}$ , (d)  $S_{21}$ , (e)  $S_{31}$ , and (f)  $S_{32}$  of an Agilent 11667B power splitter.



(f)

Fig. 4.11 Reconstructed results of (a)  $S_{11}$ , (b)  $S_{22}$ , (c)  $S_{33}$ , (d)  $S_{21}$ , (e)  $S_{31}$ , and (f)  $S_{32}$  of an Agilent 11667B power splitter.

Average errors (%)	
$S_{11}$ : 7.25	$S_{12}$ : 409.10
$S_{21}$ : 4.78	$S_{22}$ : 12.32



Table 4.5 Average errors of the third example of an amplifier.

Average errors (%)		
$S_{11}$ : 9.50	$S_{12}$ : 0.33	$S_{13}$ : 0.51
$S_{21}$ : 0.37	$S_{22}$ : 1.22	$S_{23}$ : 1.72
$S_{31}$ : 0.57	$S_{32}$ : 1.74	$S_{33}$ : 1.62

Table 4.6 Average errors of the fourth example of a three-port reciprocal DUT.



## Chapter 5 Conclusion



This dissertation describes the approach to reconstruct the  $S$ -matrices of a multiport network from a set of one-port measurements. By properly using auxiliary circuits and the type-II PRM, the  $S$ -matrix of a multiport network can be properly reconstructed. Based on the considerations of reduction of the number of one-port measurements, the accuracy of the reconstructed results and the solvability, discussion about the selection and criteria of the auxiliary circuit is also given. By properly selecting the auxiliary circuit, the  $S$ -matrices of three-port reciprocal and nonreciprocal DUTs and two-port active DUT can be reconstructed from ten one-port and five one-port measurements respectively and experimentally demonstrated. The reconstructed results are shown in close agreement with the directly measured results.

As described in Section 2.1, the number of one-port measurements to reconstruct the  $S$ -matrix of a two-port DUT is four or five. The rising curve of the number of measurements in terms of the number of DUT ports over two ports is related to that of type-II PRM being approximated to be  $3^{n-2}$ . Therefore, the number of one-port measurements for an  $n$ -port DUT involved in this study is about  $4 \times 3^{n-2}$  to  $5 \times 3^{n-2}$ . As for the number of connections, a multiport VNA for three-port measurements needs six connections including three for calibration using an E-cal kit and three for measurement. Each experiment given in this study, however, needs thirty-five connections including

three for calibration and thirty-two for one-port measurements.



The developed results given in this study imply that extra efforts are required to determine the  $S$ -matrix of an  $n$ -port DUT from one-port measurements. These efforts include the hardware/software integration and the consideration of the imperfection of cable-flex repeatability or switches in one-port measurements. For the hardware and software, one needs to integrate one-port VNA, auxiliary circuit, switches, cables and a PC with reconstruction algorithm. Short phase stable cables connecting the auxiliary circuit and the DUT can mitigate ripples occurring in the reconstructed results. As for the imperfection of switches, the mismatch and loss can be regarded as parts of the auxiliary circuit or the terminations and de-embedded. However, considering Fig. 4.1, the switch imperfect isolation will make the measured data to relate all the components involved. This then renders the one-port measurement equation to be very complicated. Although these issues have to be considered to improve the practicability of the developed approach, the presented results provide an approach to extend the application of a one-port VNA in the determination of the  $S$ -matrix of an  $n$ -port DUT.



## Appendices

### Appendix A Prove of $q / p = -(S_{12} + S_{21})$

From (12) and (15), one can have

$$\begin{aligned} p &= N_2 - BD_2 \\ q &= N_0 - BD_0 \\ r &= (N_1 - BD_1)RTP. \end{aligned} \quad (\text{A.1})$$

Substituting (7) into the first two equations in (A.1) gives

$$p = N_2 - \frac{N_0 + N_1S_{12} + N_2S_{21}}{D_0 + D_1S_{12} + D_2S_{21}} D_2 \quad (\text{A.2})$$

$$q = N_0 - \frac{N_0 + N_1S_{12} + N_2S_{21}}{D_0 + D_1S_{12} + D_2S_{21}} D_0. \quad (\text{A.3})$$

Dividing (A.3) by (A.2) gives

$$\frac{q}{p} = \frac{-(N_1D_0 - N_0D_1)S_{12} - (N_2D_0 - N_0D_2)S_{21}}{(N_2D_1 - N_1D_2)S_{12} + (N_2D_0 - N_0D_2)}. \quad (\text{A.4})$$

According to (8) and (9), if the auxiliary circuit is reciprocal, then

$$N_1 = a_{12}a_{31} = a_{21}a_{13} = N_2 \quad (\text{A.5})$$

$$D_1 = -a_{32} = -a_{23} = D_2. \quad (\text{A.6})$$

By substituting (A.5) and (A.6) into (A.4), one can prove

$$\frac{q}{p} = \frac{-(N_1D_0 - N_0D_1)S_{12} - (N_2D_0 - N_0D_2)S_{21}}{N_2D_0 - N_0D_2} = -(S_{12} + S_{21}). \quad (\text{A.7})$$

### Appendix B Prove of $r / p = S_{12}S_{21}$


By substituting (A.5) and (A.6) into (A.1), it is clear that

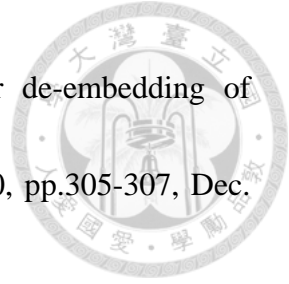
$$\frac{r}{p} = \frac{(N_2 - BD_2)RTP}{N_2 - BD_2} = RTP = S_{12}S_{21}. \quad (\text{A.8})$$

## References



- [1] M. Davidovitz, "Reconstruction of the S-matrix for a 3-port using measurements at only two ports," *IEEE Microwave Guided Wave Lett.*, vol. 5, no. 10, pp. 349-350, Oct. 1995.
- [2] J. C. Tipper and R. A. Speciale, "A rigorous technique for measuring the scattering matrix of a multi-port device with a two-port network analyzer," *IEEE Trans. Microwave Theory Techn.*, vol. MTT-30, no. 5, pp.661-666, May 1982.
- [3] J. C. Rautio, "Techniques for correcting scattering parameter data of an imperfectly terminated multiport when measured with a two-port network analyzer," *IEEE Trans. Microwave Theory Techn.*, vol. MTT-31, no. 5, pp.407-412, May 1983.
- [4] I. Rolfes and B. Schiek, "Multiport method for the measurement of the scattering parameters of n-ports," *IEEE Trans. Microwave Theory Techn.*, vol. 53, no. 6, pp.1990-1996, Jun. 2005.
- [5] S. Sercu and L. Martens, "Characterizing n-port packages and interconnections with a 2-port network analyzer," in *IEEE 6<sup>th</sup> Topical Meeting on Electrical Performance of Electronic Packaging*, pp. 163-166, Oct. 1997.
- [6] D. F. Williams and D. K. Walker, "In-line multiport calibration algorithm," in *51<sup>st</sup> ARFTG Conf. Dig.*, pp. 88-90, June 1998.

- 
- [7] W. Lin and C. Ruan, "Measurement and calibration of a universal six-port network analyzer," *IEEE Trans. Microwave Theory Techn.*, vol. 37, no. 4, pp. 734-742, Apr. 1989.
- [8] H. C. Lu and T. H. Chu, "Port reduction methods for scattering matrix measurement of an n-port network," *IEEE Trans. Microwave Theory Techn.*, vol. 48, no. 6, pp. 959-968, June 2000.
- [9] H. C. Lu and T. H. Chu, "Multiport scattering matrix measurement using a reduced-port network analyzer," *IEEE Trans. Microwave Theory Techn.*, vol. 51, no. 5, pp. 1525-1533, May 2003.
- [10] J. Martens, D. Judge, and J. Bigelow, "Multiport vector network analyzer measurements," *IEEE Microwave Magazine*, vol. 6, no. 4, pp. 72-81, Dec. 2005.
- [11] T. G. Ruttan, B. Grossman, A. Ferrero, V. Teppati, and J. Martens, "Multiport VNA measurements," *IEEE Microwave Magazine*, vol. 9, no. 3, pp. 56-69, June 2008.
- [12] A Ferrero, V. Teppati, E. Fledell, B. Grossman, and T. Ruttan, "Microwave multiport measurements for the digital world," *IEEE Microwave Magazine*, vol. 12, no. 1, pp. 61-73, Feb. 2011.



- [13] P.C. Sharma and K.C. Gupta, "A generalized method for de-embedding of multiport networks," *IEEE Trans. Instrum. Meas.*, vol. IM-30, pp.305-307, Dec. 1981.
- [14] A.Ferrero and F. Sanpietro, "A simplified algorithm for leaky network analyzer calibration," *IEEE. Microwave Guided Wave Lett.*, vol. 5, pp.119-121, Apr. 1995.
- [15] C. J. Chen and T. H. Chu, "Accuracy criterion for S-matrix reconstruction transforms on multiport networks," *IEEE Trans. Microwave Theory Tech.*, vol. 59, no. 9, pp. 2331-2339, Sep. 2011.
- [16] C. J. Chen and T. H. Chu, "Virtual auxiliary termination for multiport scattering matrix measurement using two-port network analyzer," *IEEE Trans. Microwave Theory Tech.*, vol. 55, no. 8, pp. 1801-1810, Sep. 2007.
- [17] G. F. Engen, "The six-port reflectometer: an alternative network analyzer," *IEEE Trans. Microwave Theory Techn.*, vol. MTT-25, no. 12, pp. 1075-1080, Dec. 1977.
- [18] Y. C. Lin and T. H. Chu, "Determining scattering matrix of a three-port reciprocal network from one-port measurements," in *Asia Pacific Microwave Conference Digest*, pp. 432-434, Nov. 2014.
- [19] M. Abramowitz and I. A. Stegun, *Handbook of Mathematical Functions with Formulas, Graphs, and Mathematical Tables*, pp. 17, New York: Dover, 1972.